Precambrian Geology of the Northern Part of the Los Pinos Mountains, New Mexico

by

Kenneth M. Mallon

Submitted to the Geology Department
The New Mexico Institute of Mining and Technology
in partial fulfillment of the requirements
for the degree of
Master of Science in Geology

Submitted May 20, 1966.

Opposite page: view of the western face of the northern part of the Los Pinos Mountains, New Mexico.

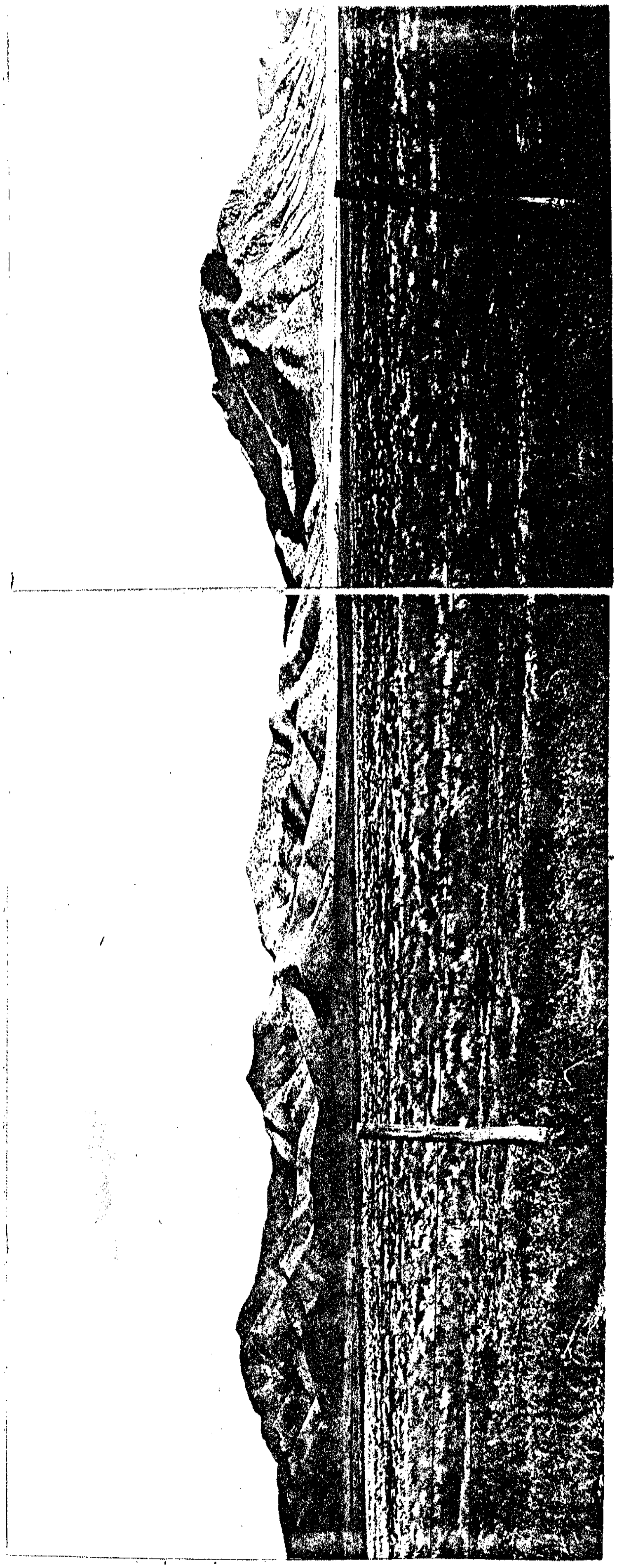

CONTENTS

ABSTRACT 1

INTRODUCTION 3

Previous Work 3

Location, Extent and Access 3

Geologic Setting and Physical Features 4

Methods of Study 7

Acknowledgements 8

POST-PRECAMBRIAN GEOLOGY 9

Quaternary 9

Pennsylvanian 9

Post-Metamorphism, Pre-Pennsylvanian 9

PRECAMBRIAN GEOLOGY 11

Petrology 11

INTRODUCTION 11

LEPTYNOLITE 12

FELDSPATHIC QUARTZ-MUSCOVITE-CHLORITE AND FELDSPATHIC QUARTZ-MUSCOVITE-BIOTITE SCHIST AND PHYLLITE 17

MUSCOVITIC QUARTZITE 22

GRANITIC GNEISS 29

HORNBLENDE-CHLORITE SCHIST 35

METAMORPHISM 40

First Deformation 42

Thermal Metamorphism 43

Second Deformation 46

Retrograde Effect 47

Third Deformation-Dislocation Metamorphism 47
METAMORPHIC FACIES CLASSIFICATION 48
PARENT ROCKS 52
Structural Geology 57
INTRODUCTION 57
PRE-FIRST DEFORMATION 58
FIRST DEFORMATION 59
Microscopic Structures 59
Mesoscopic Structures 60
Folds 60
Planar Structures 65
Quartz Layers 66
Linear Structures 67
Boudins 68
SECOND DEFORMATION 69
Microscopic Structures 69
Mesoscopic Structures 70
Folds 70
Planar Structures 76
Linear Structures 77
THIRD DEFORMATION 78
Microscopic Structures 78
Mesoscopic Structures 79
Planar Structures 79
Linear Structures 79
JOINTS 80

SUMMARY OF STRUCTURAL GEOLOGY 81

GEOLOGIC HISTORY 84

GLOSSARY 85

BIBLIOGRAPHY 87

ILLUSTRATIONS

TABLES

I. Equilibrium assemblages of regional metamorphism in the northern part of the Los Pinos Mountains 50

II. Summary of Structural History 82

FIGURES

1. Index map 5

2. Typical outcrop of leptynolite 16

3. Lepidoblastic texture in leptynolite defined by biotite flakes 16

4. Looking NE from White Ridge into valley cut in feld spathic quartz-muscovite-biotite (and chlorite) schist 20

5. Crinkled S_1 flow cleavage; segregation layers of micas and quzrtzo-feldspathic areas 20

6. Large "layered" outcrop of muscovitic quartzite... 23

7. Steep fracture cleavage dip slope of muscovitic quartzite forms the western side of White Ridge... 23

8. Cataclastic textures in muscovitic quartzite 26

9. Micas defining flow cleavage are completely enclosed within optically continuous quartz grains..... 26

10. Granitic gneiss outcrop showing wide-spaced cleavage 32

11. Graphic intergrowth of quartz and feldspar bordering a feldspar grain 32

12. Myrmekitic and graphic intergrowths bordering quartz and feldspar grains 33

13. Odd-shaped quartz-microcline perthite intergrowth in granitic gneiss 33

14. Interlayers of hornblende-chlorite schist in leptynolite 37

15a. Biotite porphyroblasts poikiloblastically include grains that define S_1 flow cleavage; biotite grains are bent and sheared by D_2 cleavage 45

15b. Sketch of Figure 15a. indicating structural elements 45

16. Projection drawing of F_1 microfold 61

17. Isoclinal F_1 flow fold of hematite and magnetite rich layer in muscovitic quartzite 61

18. F_1 shear fold in muscovitic quartzite with sheared out axial plane 63

19. Biotite layers in feldspathic quartz-muscovite-biotite schist forming F_1 shear folds with S_1 axial plane flow cleavage 63

20. F_1 crinkle folds in schist 64

21. F_1 folds in schist; light colored layers are quartz rich. S_1 axial plane cleavage cuts fold limbs and nose 64

22. Successive stages, from A to C, in the formation of close-spaced S_2 slip cleavage..... 71

23. F_2 assymmetrical folds with poorly developed axial plane cleavage in muscovitic quartzite; folded element is S_1 axial plane cleavage..... 73

24. F_2 chevron cleavage folds folding S_1 in feldspathic quartz-muscovite-biotite schist 73

25. Quartz layer defining F_2 folds in schist. S_2 axial plane cleavage is so well-developed in places that the folds are no longer recognizable 74

26. F_2 antiform-synform pair in muscovitic quartzite... 74

27. Broad F_2 flexure fold in muscovitic quartzite with incipient development of axial plane cleavage 75

28. Rare F_2 fold in leptynolite; the fold has a crumpled and sheared axial area 75

PLATES

I. Geologic and Structural Map ..... in pocket

Ia. Thinsection location map (overlay for Plate I) " "

II to VIII. Lower hemisphere equal area stereographic projections of structural data (point diagrams) "

ABSTRACT

Precambrian rocks in the northern part of the Los Pinos Mountains have been modified by three periods of metamorphism . The most prominent feature of the earliest recognizable deformation is cataclastic texture; relict cataclastic textures are recognizable in all rocks. This earliest regional metamorphism produced isoclinal shear and flexure folds with penetrative axial plane flow and fracture cleavage that contains prominent textural and mineralogic lineation parallel to fold axes. First deformation fold axes trend N 50°-70° W, and plunge 50°-70° NW. A second deformation has folded first deformation axial plane cleavage into symmetrical and assymmetrical flexural slip and cleavage folds with axes that range in trend from N 25° E, through North, to S 15° W; the plunge has a range of 35°-60° northward and westward. A third period of deformation has produced homogeneous, non-penetrative, east-west trending fracture cleavage which transects first and second deformation axial plane cleavages.

The major metamorphic rock types are muscovitic quartzite, biotite and chlorite schist and phyllite, leptynolite or feldspathic schist, granitic gneiss, and hornblende-chlorite schist. Quartzose and pegmatitic veins, layers and boudins are common in most units and have been affected by three deformations. The earliest metamorphism resulted in the formation of quartzite, schist and gneiss from original impure quartz sandstone, impure shale, granitic rocks or

granitized sediments, and possibly some intercalated flow rocks. Equilibrium mineral assemblages formed during the first metamorphism are characteristic of the greenschist and almandine-amphibolite facies of regional metamorphism. Thermal metamorphism following the first metamorphism is marked by the recrystallization of large grains of biotite and chlorite which poikiloblastically include first deformation textures. Structures related to the second and third deformations deform or transect minerals formed during the thermal metamorphism.

INTRODUCTION

This study of the northern part of the Los Pinos Mountains elucidates the sequence of tectonic and petrologic events which has affected the Precambrian rocks of this area. The principal means of interpreting the tectonic history has been the systematic collection and study of data concerning the attitude and style of small scale structures.. Most of the petrologic conclusions have been based on data obtained from the study of thinsections.

Previous Work

The only published report on the Precambrian geology of the Los Pinos Mountains appears in Stark and Dapples (1946), but this study was mostly concerned with stratigraphy. The structural complexity of the area was not recognized. Structural elements were interpreted as primary sedimentary structures or were related to one period of metamorphism. The only other work in the area was by Staatz and Norton (1942, unpublished M.S. thesis, Northwestern University). However, the present writer was not able to obtain this thesis from Northwestern.

Location, Extent and Access

The Los Pinos Mountains are located in Socorro County, New Mexico, about 31 miles northeast of Socorro, New Mexico,

and 27 miles southeast of Belen, New Mexico (see Fig. 1-Index Map). The mountain range lies between the latitudes of 34° 16' and 34° 27' north. The entire range extends for about 15 miles and trends S 20° W. The northernmost nine square miles of exposed Precambrian rocks were mapped.

Easy access to the northern part of the mapped area is provided by a dirt and gravel road which extends through Goat Draw to Goat Ranch. The road is accessible by passenger car except when heavy summer rains produce runoff that inundates Goat Draw. The eastern and southeastern parts of the map area are served by a graded dirt road which extends from U.S. Highway 60 to the Parker Ranch. White Sands Missile Range road #3 extends southward from U.S. Highway 60 past Torotutu Butte which is a few miles west of the mountain range. A graded gravel road and a network of unimproved dirt roads (not accessible by passenger car) extend from the Missile Range road to various parts of the range front and to the unoccupied Burris ranch house. All the roads that provide access are on private property and are closed by locked gates except the Parker Ranch road.

Geologic Setting and Physical Features

The Los Pinos Mountain range is the southernmost of three physiographically similar and northerly extending mountain ranges in central New Mexico. The Los Pinos

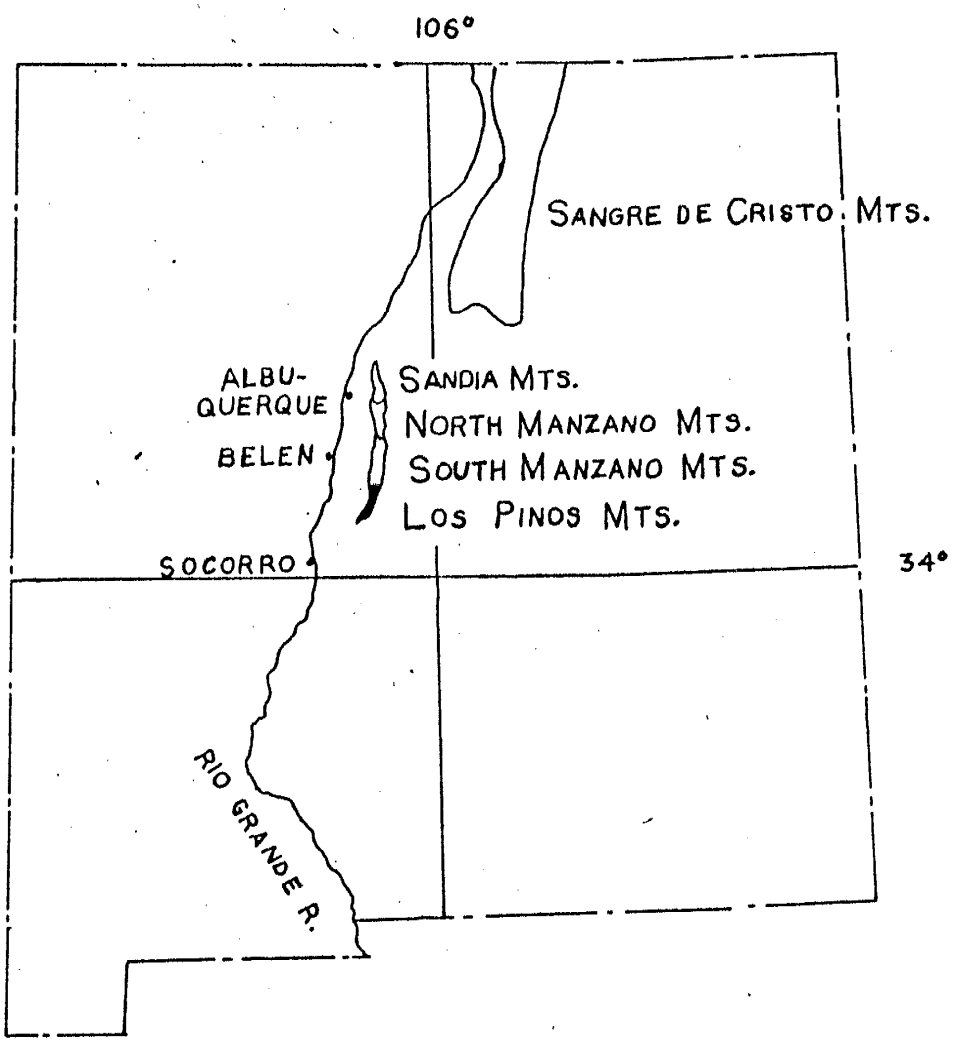

Figure 1. Index map of New Mexico showing the location of the Los Pinos Mountains.

Mountains in part have a steep western face and a gentle slope, just as the two ranges to the north, the Sandia Mountains and the Manzano Mountains. Part of the western face of the range is a fault scarp probably related to the Rio Grande graben structure, the easternmost fault structure of the Basin and Range Province. The mountains are bordered on the west by the Tio Bartolo Pediment (Denny, 1941). The range is bounded on the east by the Montosa thrust which has placed Precambrian metamorphic rocks adjacent to Pennsylvanian sediments. In the southern part of the range the Pennsylvanian sediments lie unconformably on the Precambrian. The sediments presumably at one time completely covered the Precambrian rocks, which have since been exposed in the northern part of the Los Pinos Mountains by erosion.

Topography of the region is generally rugged; it is subdued only in Goat Draw where micaceous rocks are exposed. The maximum relief is 1980 feet, in the southern part of the map area. Much of the topography consists of steep-sided hills and ridges. Prominent topographic highs are Whiteface Mountain which consists of granitic gneiss, and White Ridge which extends almost the entire length of the central part of the map area and is underlain by muscovitic quartzite.

The stream pattern is radial in the vicinity of granitic gneiss, but becomes trellis-like within the mountain range.

The pattern of streams draining onto Tio Bartolo Pediment is dendritic. Streams generally flow westward from the west side of White Ridge and eastward to northwastward from the east side of the ridge. All streams in the valley east of White Ridge drain northward via Goat Draw, except for a few streams in the southern part of the map area which drain eastward through narrow gaps in a ridge formed by upturned beds of Paleozoic sediments. Vegetation consists of various cacti, pinon and sparse grass.

Methods of Study

The Precambrian rocks within nine square miles of the northern Los Pinos Mountains were mapped at a scale of 1:16,620 using aerial photographs supplied by the State Bureau of Mines and Mineral Resources, Socorro, New Mexico. Geology was later transposed to an enlarged United States Geological Survey $7\frac{1}{2}$ minute topographic map of Becker Quadrangle, New Mexico.

Forty-five days were spent in the field during the summer and fall of 1965. The attitude and style of small scale structural features were recorded at more than 700 outcrop stations. Fifty-one thinsections were studied. The locations of thinsection samples are shown in Plate Ia.

Acknowledgements

The writer expresses his appreciation to Dr. E.C. Bingler for introducing him to the area, for the many profitable discussions regarding structural features and interpretations, and metamorphic petrology, and for his unceasing aid and advice in the preparation of the manuscript. Sincere appreciation goes to Dr. C.T. Smith and Mr. Max E. Willard for suggestions and critical review of the manuscript. Some of the technical problems encountered in the study were profitably discussed with Drs. J.R. Renault, A.L. Albee and J. Wasserburg.

Special thanks are due Mr. A.J. Thompson, Director of the State Bureau of Mines and Mineral Resources, who provided finandial aid to defray the cost of preparation of thin-sections. Sincere gratitude is due the New Mexico Geological Society which awarded the author a Grant in Aid to defray the cost of field expenses. Thanks are also due Mr. Max Miranda, R.L. Parker and especially Weldon Burris who gave permission for the use of their private roads. Mr. Burris provided keys for many of the locked gates on his property.

Finally, thanks go to my wife Mary Lynn for helping with the typing of the manuscript and preparation of the maps.

POST-PRECAMBRIAN GEOLOGY

Quaternary

No detailed study of the Tio Bartolo Pediment (Denny, 1941) has been made. The pediment gravels have been included with stream alluvium and talus and mapped as Qal in this study.

Pennsylvanian

Limestone beds, generally one to three feet thick, crop out along the eastern border of the map area. The rock is gray to yellow-brown, fine-grained, and has a hackly texture. The beds have been thrown into drag folds as a result of thrust faulting. A few dip and strike measurements have been taken on this rock unit.

Post-metamorphism, Pre-Pennsylvanian

Two conglomerate exposures of small areal extent have been mapped within the Precambrian exposures. One conglomerate crops out in the eastern belt of muscovitic quartzite (Plate I) and consists of fragments of leptynolite, feldspathic quartz-muscovite-chlorite and feldspathic quartz-muscovite-biotite schist and phyllite, and muscovitic quartzite. The exposure is angle-shaped and is 1/4 to 1/3 mile long and 200 to 300 feet wide. Outcrops are subdued. The rock fragments are angular to sub-rounded and range in

size from a few millimeters to a few feet. They are set in a reddish-brown, submicroscopic to fine-grained matrix consisting of magnetite, hematite, chlorite, calcite, quartz, feldspar and white mica.

The other exposure is in the extreme southern part of the map area in the leptynolite belt. The outcrop area is 1/8 mile long and 30 to 60 feet wide. Outcrops are very subdued and are gray to tan in color. The conglomerate consists essentially of quartz and feldspar grains with minor amounts of muscovite, chlorite, biotite, magnetite, zoisite and myrmekite. Hematite, zircon and sphene are accessories. Feldspars include microcline and microcline perthite. Some quartz grains are as large as 2.5mm in diameter, but the average grain size is 0.05mm to 1.5mm. A few angular fragments of muscovitic quartzite and leptynolite are present and are generally 2mm to 3mm in diameter. This unit shows incipient fracturing which trends N 30° E and dips steeply. The two conglomerates apparently were deposited on the exposed Precambrian surface before deposition of the Pennsylvanian limestone. On the Geologic Map (Plate I), both exposures are shown by the symbol cgl.

PRECAMBRIAN GEOLOGY

Petrology

INTRODUCTION

The northern part of the Los Pinos Mountains consists essentially of Precambrian metamorphic rocks. The metamorphic units are separated and mapped on the basis of lithology and texture. The major rock units thus established are muscovitic quartzite, feldspathic quartz-muscovite-chlorite and feldspathic quartz-muscovite-biotite schist and phyllite, leptynolite, granitic gneiss and hornblende-chlorite schist.

General characteristics of all the units include (1) a high silica content as indicated by the presence of quartz in all the rocks except a few scattered samples of hornblende-chlorite schist; (2) fine-grained feldspar present in the rocks except for a few samples of hornblende-chlorite schist and the majority of the muscovitic quartzite (only the western part of the muscovitic quartzite exposure contains feldspar, and this variant is actually gradational into leptynolite to the west ; (3) the fine-grained nature of all the rocks. Except for the large quartz and feldspar grains in leptynolite and the feldspathic variant of muscovitic quartzite, the grain size of the rocks is generally less than 0.15mm. Leptynolite is the most fine-grained rock in the map area; grains are often submicroscopic.

All rock units except the granitic gneiss crop out in belts trending approximately N 20°-30° E. Granitic gneiss crops out in an irregular pattern in the southwestern part of the map area. The rock units are discussed below in approximate order of their areal extent; the most extensive unit is discussed first and the least extensive unit is discussed last. Average compositions of the units have been estimated visually.

LEPTYNOLITE

Leptynolite is a very fine-grained granulitic rock composed mainly of quartz and felspar with a minor amount of mica; the rock texture is generally slightly fissile. This name is here given to the rock unit which Stark and Dapples (p. 1134) named Sevilleta Rhyolite. Leptynolite has been chosen because it best fits the lithology and texture of this unit.

Leptynolite crops out in a belt 3/16 to 1 1/4 miles wide and 4 miles long along the western side of the northern part of the Los Pinos Mountains. The unit is bounded on the west by a normal fault, on the east by muscovitic quartzite and partially on the south by granitic gneiss. The leptynolite-muscovitic quartzite contact is gradational. The percentage of large quartz and feldspar grains set in the fine-grained matrix of the rock decreases gradually toward the east and toward the muscovitic quartzite. The

matrix of the rocks becomes less feldspar-rich and more quartz-rich toward the muscovitic quartzite exposures. Sparse outcrops are generally restricted to arroyos and hilltops. Leptynolite is generally well-cleaved and rarely massive (Fig. 2). In places the rocks are so well cleaved in two or three directions that cleavage fragments resemble those of pencil shale.

Leptynolite is brownish-red to red-orange on weathered surfaces. This coloring imparts a red-orange appearance to the soil adjacent to the rocks. The red-orange color becomes less noticeable to the east toward the muscovitic quartzite exposures. The rock is gray to grayish white on fresh surfaces. The rocks generally have a dull luster and poorly developed schistosity. Some samples have a silky luster and well developed schistosity. Schistosity always contains prominent textural and mineralogic lineation. Laminae of variable composition are present but rare. Black, brown and dark green layers less than 1/8 inch to 1/4 inch thick are composed of biotite, specular hematite, and magnetite; these laminae are parallel to the prominent northeast trending schistosity in the rock. Pink feldspar-rich laminae less than 1/4 inch thick occur slightly to complexely folded; the northeast trending schistosity transects the laminae and is axial plane cleavage to the folds. A few layers of feldspathic quartz-muscovite-biotite schist as thick as 250 feet are present in the eastern portion of

the leptynolite belt.

The average composition of leptynolite is 55% quartz, 25% feldspar, 7% muscovite, 7% biotite and 3% chlorite. Anhedral to subhedral laths of feldspar as long as 13mm but commonly 2mm to 4mm long are set in a fine-grained matrix of quartz, feldspar and mica. Average grain size of matrix grains ranges from 0.025mm to 0.12mm. Large rounded quartz grains with undulatory extinction are also set in the matrix. These quartz grains are generally about 8mm to 16mm in diameter. Some of the large quartz grains are elongate in the plane of schistosity. A few samples show phacoidal areas 8mm to 10mm long and 3mm to 5mm wide composed of numerous small granoblastic quartz grains. Matrix feldspar is generally albite, about 60% untwinned and 40% twinned, but microcline and orthoclase(?) are also present. Large feldspars are albite and microcline perthite, but microcline is present. Rare plagioclase grains exhibit metamorphic zoning. A few myrmekitic intergrowths of quartz and perthite are present. Alteration products include white mica and calcite replacing feldspar. Calcite is the most common and is often present as pseudomorphs after large feldspar grains. Pseudomorphs of limonite after pyrite, 1/16 inch to 3/4 inch in diameter, occur in a few thinsections. Antigorite rarely occurs as an alteration of chlorite. Most thinsections contain a few grains of twinned and untwinned cordierite. Accessory

minerals include zoisite, which forms bladed crystals and rosettes, hematite, magnetite, apatite, sphene, zircon, greenish gray tourmaline and rare pink garnet.

The lepidoblastic texture in this rock is a flow cleavage marked by minute (0.025mm to 0.075mm) flakes of muscovite, chlorite and dark brown to green biotite with a high degree of preferred orientation (Fig. 3). Later slip cleavage deforms the flow cleavage in some samples. Where mica is too scarce to form flow cleavage, a close-spaced fracture cleavage is present and has the same orientation as the flow cleavage. Flow cleavage generally envelops large quartz and feldspar grains, although some mica that defines flow cleavage is completely enclosed within optically continuous quartz grains. Incipient fracture cleavage cuts flow, slip and fracture cleavages and occurs approximately perpendicular to flow cleavage. Coarse-grained stringers and anastomosing veinlets of minute quartz grains are present in leptynolite.

Leptynolite becomes slightly coarser-grained and contains less large quartz and feldspar grains near the contact with muscovitic quartzite. Close to the contact with granitic gneiss leptynolite is irregularly altered and the northeast trending schistosity occurs as zones three to five feet wide alternating with less schistose zones of similar dimensions. Frequency of occurrence of large feldspar grains increases toward granitic gneiss exposures. This

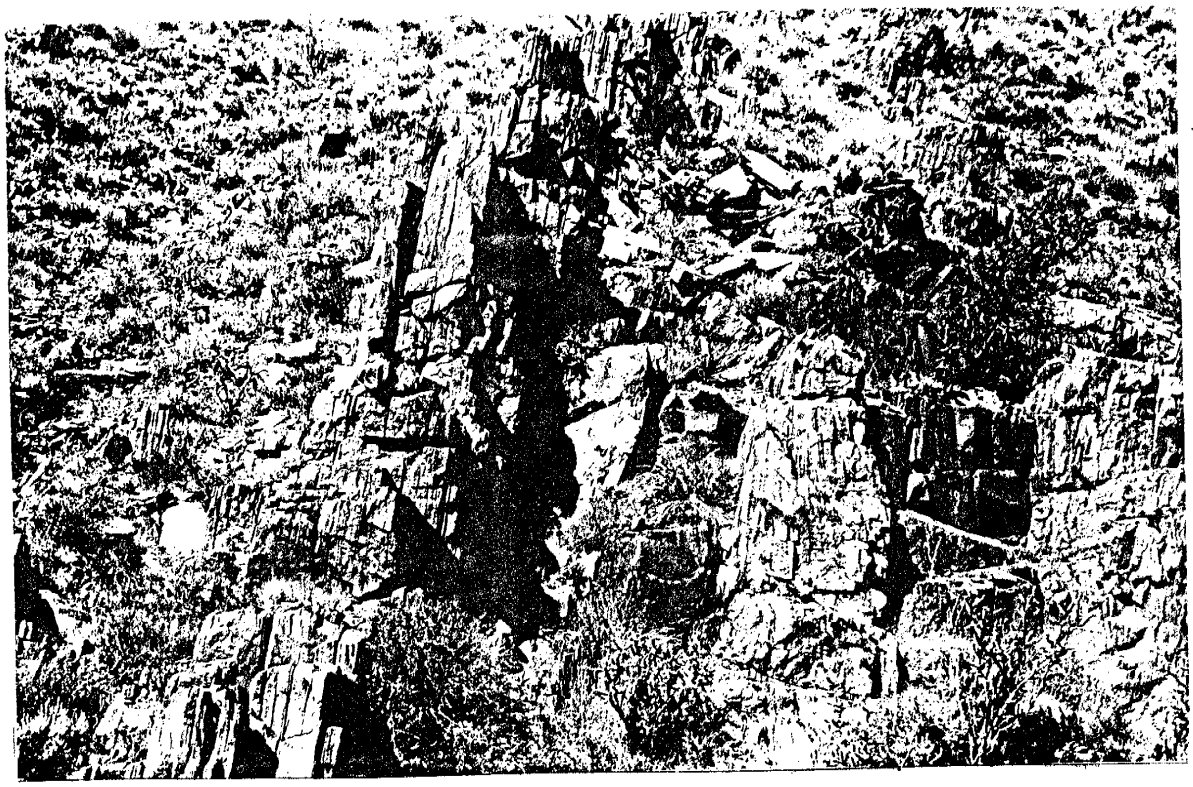

Figure 2. Typical outcrop of leptynolite; note several cleavage directions.

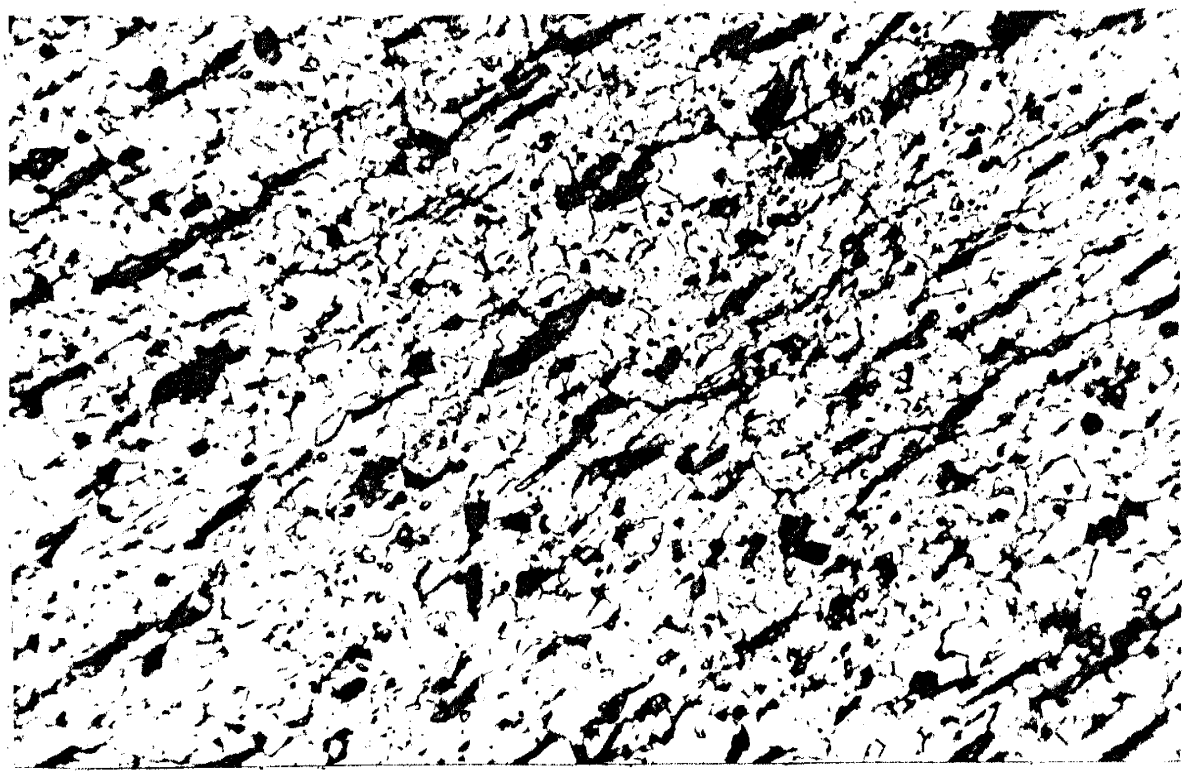

Figure 3. Lepidoblastic texture in leptynolite defined by biotite flakes (X120).

is characteristic not only of the leptynolite-granitic gneiss contact area but also of scattered outcrops which have no ordered arrangement except that they are located in the eastern portion of the leptynolite belt.

A rock compositionally and texturally similar to leptynolite is inter-layered with feldspathic-quartz-muscovite-chlorite and feldspathic-quartz-muscovite-biotite schist in the valley east of White Ridge. These interlayers are generally less than 15 feet thick and are composed of about 50% quartz, 40% feldspar and a few percent muscovite and biotite. A vague layering defined by grain size variation is present; this might suggest a clastic origin for the rock. This rock differs from leptynolite only in the absence of large quartz and feldspar grains.

Boudins and irregular vein-like masses of milky quartz are present throughout the leptynolite belt. In the southern part of the leptynolite area the vein-like masses of quartz contain coarse-grained orange-pink K-feldspar. The K-feldspar content increases in a southerly direction toward the granitic gneiss exposures. Irregular masses of epidote are present in leptynolite but occur more sporadically than quartz masses.

FELDSPATHIC-QUARTZ-MUSCOVITE-CHLORITE and FELDSPATHIC-QUARTZ-MUSCOVITE-BIOTITE SCHIST and PHYLLITE

Schist and phyllite composed of muscovite, quartz, feldspar, chlorite and/or biotite constitute about 20 to 25%

of the map area. The principal outcrop pattern is a belt approximately three miles long and 1/3 to 3/4 mile wide (Plate I) which is topographically a valley (Fig. 4). The main schist outcrop area is bounded on the east and west by muscovitic quartzite; both contacts are folded. A few continuous layers of the schist, as thick as 350 feet but usually 30 to 100 feet thick, crop out in the central muscovitic quartzite belt and the leptynolite belt. Exposures are not abundant except on White Ridge where the schist and phyllite crop out almost continuously along the length of the ridge. Typical outcrops of this unit in the valley are very subdued, generally being only a few inches above the ground. The best outcrops in the valley are found in shallow arroyos.

Feldspathic quartz-muscovite-chlorite and feldspathic quartz-muscovite-biotite schist and phyllite are generally greenish-gray to blue-gray on weathered surfaces, but buff to orange varieties colored by hematite are present. Fresh surfaces are blue-gray. This unit commonly has a very silky luster due to the parallel arrangement of muscovite flakes. All outcrops exhibit well-developed schistosity, and many outcrops show additional slip cleavage and isoclinal folding. Prominent textural and mineralogic lineations are always present and occur in the schistosity planes.

The average composition of this unit is 45% muscovite, 35% quartz, 7% chlorite, and 3% feldspar (albite and micro-

cline perthite). Where biotite is present in place of chlorite it constitutes 7% of the rock. Kaolin replacing feldspar is present in very small amounts. Minor constituents include magnetite, zoisite, epidote and garnet. Kyanite occurs in one sample as one or two idiomorphic grains 2.5mm long and 0.6mm wide. Accessories include blue-gray tourmaline, sphene, specular hematite, zircon and apatite.

The microscopic texture of these fine-grained crystalline rocks is mainly lepidoblastic, with flakes of muscovite and biotite or chlorite less than 0.025mm to 0.15mm long forming the well-developed flow cleavage. Flow cleavage is commonly flexed by later slip cleavage (Fig. 5). Incipient fracture cleavage occur at about 90° to the flow cleavage. Very fine laminae of micaceous minerals alternate with laminae of granoblastic quartz and feldspar grains that range from 0.05mm to 0.3mm in diameter (Fig. 5). Most of the thin-sections contain lenses or stringers of coarse-grained quartz within a fine-grained quartz-feldspar matrix. Most of the feldspar is albite, twinned according to the Albite law, but Carlsbad-Albite twins are present. Untwinned albite, microcline perthite and rarely K-feldspar (orthoclase?) are all present. The flow cleavage transects and shears out some feldspar grains, but envelops others, especially some larger feldspar grains that attain a diameter of 2.0mm. Most feldspar grains are free of inclusions, but some are dusty with inclusions of zircon and apatite. Some feldspar

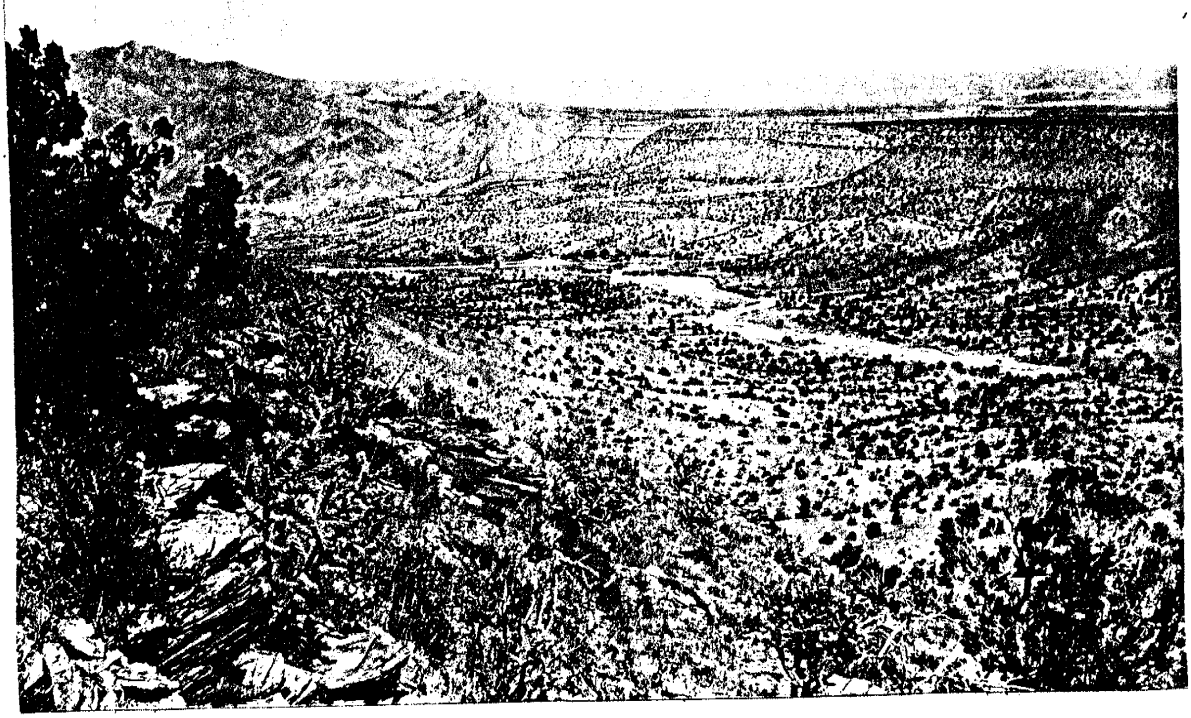

Figure 4. Looking northeast from White Ridge into valley cut in feldspathic quartz-muscovite-chlorite and feldspathic quartz-muscovite-biotite schist.

Figure 5. Crinkled S_1 flow cleavage; segregation layers of micas and quartzo-feldspathic areas (X 160).

grains poikiloblastically include magnetite, zoisite, biotite and muscovite. Textural evidence indicates that some of the biotite in the rock has apparently been changed to chlorite, but this relation is not clearly evident in all the samples. Many biotite flakes have chlorite edges and patches of chlorite in the central part of the grain. In many thinsections biotite and chlorite flakes are transverse to the slip cleavage and are cut by it. Large biotite flakes commonly show pleochroic haloes around minute zircons. Occassionally the schist and phyllite contain as much as 10% magnetite, present as euhedral and irregular grains 0.5mm to 3.0mm in diameter generally scattered throughout the rock, but rarely dispersed in thin layers.

2982 9

One outcrop located in an arroyo approximately 1/2 mile S 20° W of Goat Ranch (sample #333, Plate Ia) consists of garnetiferous quartz-muscovite-biotite schist. Almandine(?) as pink and colorless idiomorphic crystals 0.075mm to 0.4mm in diameter forms about 5% of the rock. Flow cleavage envelops the garnet porphyroblasts. A few euhedral pyrite crystals are present; pyrite crystal outlines cut across the schistosity planes.

Feldspathic quartz-muscovite-chlorite and feldspathic quartz-muscovite-biotite schist and phyllite have been named the Blue Springs Schist by Stark and Dapples (1946, p.1130).

Boudins and irregular masses of milky quartz are common in this unit. Quartz also occurs as segregations in many fold noses and axial areas of folds in the schist and phyllite.

MUSCOVITIC QUARTZITE

Muscovitic quartzite crops out in belts in the central and eastern parts of the mapped area (Plate I). The central belt is approximately 4 miles long and ranges from 1/3 to 1/4 mile wide in the north and 3/4 to one mile wide in the central and southern parts of the area, diminishing to about 1/2 mile wide near the granitic gneiss exposure. The eastern outcrop area, which is adjacent to the Montosa Thrust, is about 2 1/2 miles long and averages 1/4 mile wide.

This rock unit generally forms steep-sided ridges, e.g. White Ridge (Plate I) and hills, with numerous extensive and continuous outcrops, especially in the central belt. Outcrops in the eastern belt are not as numerous and are somewhat subdued. White Ridge, which extends almost the entire length of the central map area and trends approximately N 20°-25° E, is underlain by muscovitic quartzite. The eastern face of the ridge is generally very steep, and large "layered" masses of quartzite crop out here (Fig. 6). The western slopes of White Ridge are fracture cleavage dip slopes in muscovitic quartzite (Fig. 7).

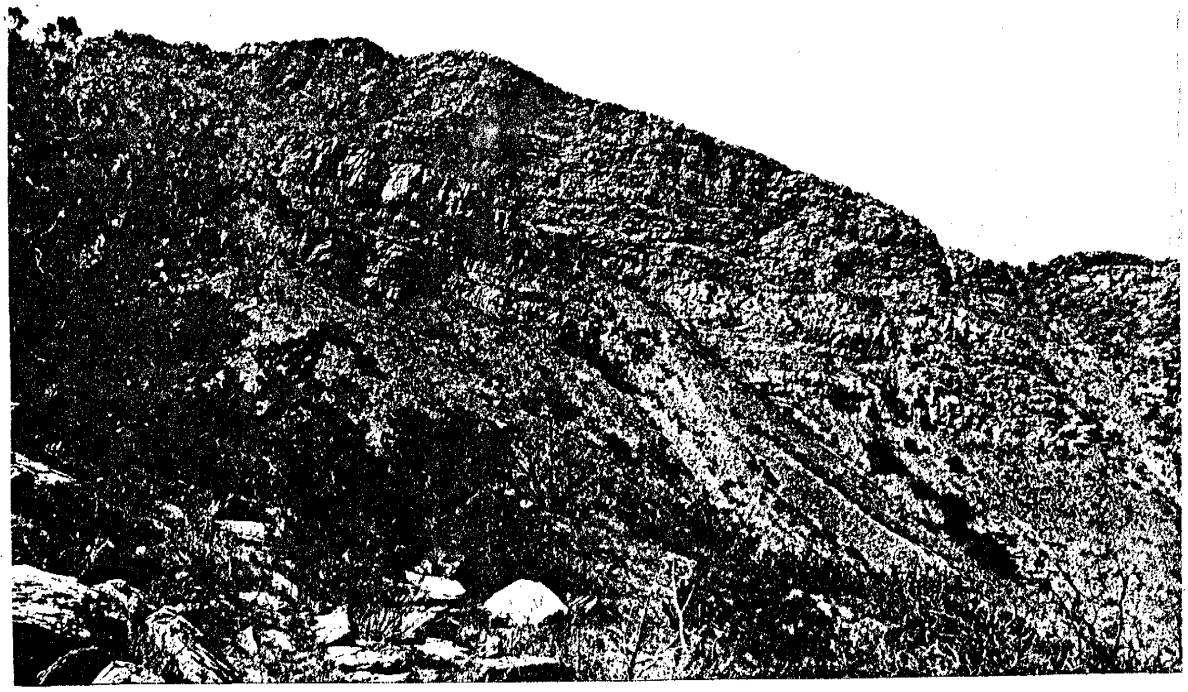

Figure 6. Large "layered" outcrop of muscovitic quartzite.

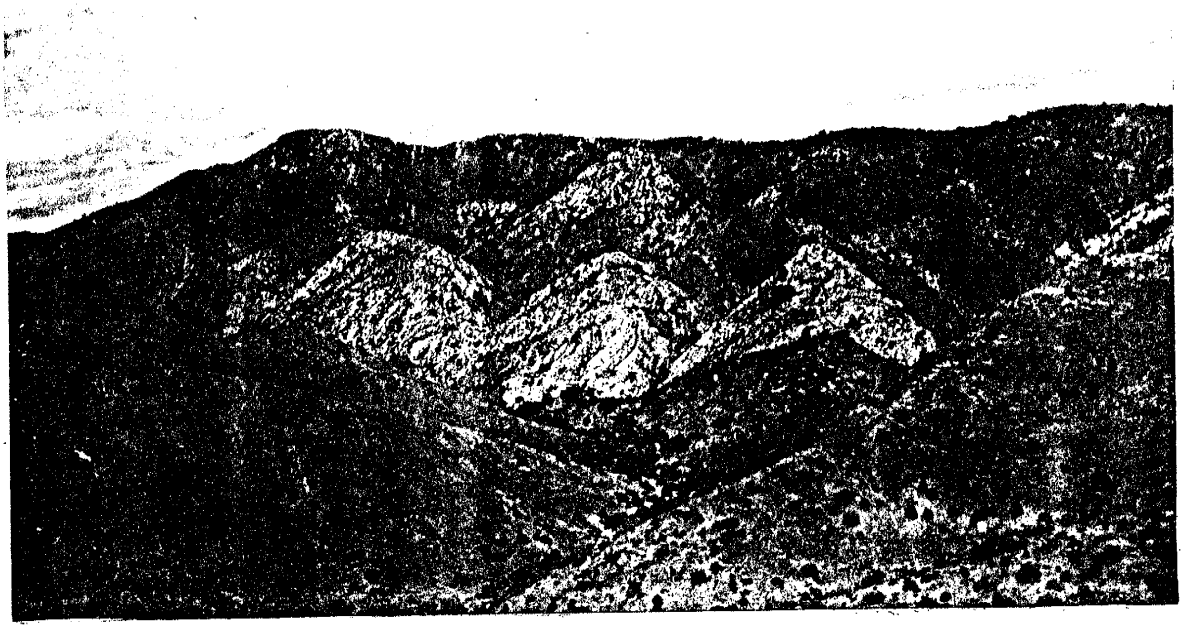

Figure 7. Steep fracture cleavage dip slope of muscovitic quartzite forms the western side of White Ridge.

Muscovitic quartzite is generally white to grayish white, but pink, purple and buff varieties colored by hematite are common. The rock has a vitreous luster due to the parallel development of micas and possibly due to the crystalline nature of the rock. Principal constituents of this fine-grained rock are quartz, muscovite and some biotite (rarely chlorite is present and not biotite). Lamination and layering are well-developed, individual layers ranging from less than 1/16 inch to ten feet thick. Thin (less than 1/25 inch to 2/3 inch) black layers that consist of specular hematite, magnetite and biotite are present; these layers commonly occur in groups three to four inches wide alternating with layers of pure quartzite. The layers are commonly tightly folded. Fracture cleavage is well-developed, with cleavage planes ranging from less than 1/16 inch to six inches apart, the majority of them 1/16 inch to 1/2 inch apart. A prominent textural and mineralogic lineation is present in the cleavage planes.

The microscopic texture is lepidoblastic and cataclastic. Common indicators of the latter are sutured grain boundaries, undulatory extinction and mortar texture (Fig. 8). Flow cleavage is defined by minute muscovite flakes with a high degree of preferred orientation. These oriented micas are commonly completely included within optically continuous quartz grains (Fig. 9). Where micas are absent, the principal planar structure is a close-spaced fracture

cleavage. Elongate quartz grains are commonly aligned with their long axes parallel to the flow or fracture cleavage (Fig. 8). A few thinsections show quartz and mica segregated into layers. Incipient fracture cleavage oriented at about 90° to the prominent flow and fracture is common. An interesting feature of the strained quartz grains of this unit is their biaxial nature. Many of these grains show biaxial + interference figures with a 2V angle as high as 20° to 25°.

The average composition of muscovitic quartzite is 80-90% quartz, 5-10% muscovite and a few percent feldspar (microcline perthite, albite and K-feldspar). The average grain size ranges from less than 0.025mm to 0.2mm, with quartz grains generally five to ten times larger than muscovite grains. Quartz grains sometimes attain a diameter of 1.5mm. Some feldspars are slightly altered to white mica. Minor constituents include chlorite, zoisite, and brownish green biotite; some zoisite prisms are 2.5mm long and 0.8mm wide. Cordierite in very minor amounts has been identified optically, but this identification has not been verified by X-ray techniques. Accessory minerals are apatite, sphene, specular hematite, zircon, blue-gray tourmaline, pink garnet and magnetite.

The contact between muscovitic quartzite and the schist and phyllite to the east is folded. Toward the western boundary of muscovitic quartzite large pinkish white

Figure 8. Cataclastic textures in muscovitic quartzite: mortar texture, sutured grain boundaries, and undulatory extinction. Quartz grains are elongate in the direction of fracture cleavage (X160; X-nicols).

Figure 9. Micas defining flow cleavage are completely included within optically continuous quartz grains (X450; X-nicols).

feldspars become evident in hand specimens. Extremely large quartz grains (superindividuals) are also common in this area. Quartz and feldspar blebs attain diameters of 3mm to 6.5mm. Some of these blebs are stretched out parallel to the prominent northeast trending rock cleavage. The large grains are set in a fine-grained matrix which consists mostly of quartz, but has feldspar and mica. Muscovitic quartzite gradually becomes finer-grained to the west and begins to contain appreciable amounts of matrix feldspar. Some of the large feldspar grains have granulated margins, but the grains are mostly subhedral to euhedral and show no evidence of granulation. This feldspathic variant of muscovitic quartzite in the western part of the outcrop belt is gradational into leptynolite.

The eastern belt of muscovitic quartzite has rocks that are compositionally similar to those in the central belt, except that biotite is less abundant, and chlorite constitutes up to 12% of the rock in places. Zoisite is also more abundant and occurs as nematoblastic prisms, radiating groups of prisms and anhedra. A few thinsections from the northern part of the belt show zoisite and quartz in segregation bands 1mm to 5mm wide, trending parallel to the prominent cleavage in the rock. The western contact of this unit with the schist and phyllite in the valley is folded. To the east the muscovitic quartzite is bounded by the Montosa Thrust.

An extremely mylonitized variety of nearly pure quartzite occurs along the eastern border of the eastern belt of muscovitic quartzite. The well-developed mylonitic textures of this rock and its restricted location along the Montoas Thrust suggest that it could be genetically related to the thrust.

A quartz-chlorite-zoisite schist from the eastern muscovitic quartzite area contains elliptically shaped, decussate clots of chlorite flakes which define a schistosity. Some of the chlorite is altered to antigorite.

Interlayers of feldspathic-quartz-muscovite-biotite schist and phyllite range in thickness from a few inches to ten feet. Accessory magnetite is common but some samples contain up to 7% magnetite euhedra usually irregularly dispersed throughout the matrix of the rock. Well-developed flow cleavage in these interlayers is marked by mica, especially muscovite, which displays a high degree of preferred orientation. Flow cleavage envelops large magnetite crystals.

Pyrite occurs in cleavage planes at several localities in both muscovitic quartzite belts. The largest cubes are 5mm to 13mm in diameter and occur in the eastern belt. Boudins and irregular masses of milky quartz are common in muscovitic quartzite.

Stark and Dapples named the rocks in the central belt the White Ridge Quartzite (p.1133), and those in the eastern

belt the Sais Quartzite (p. 1127).

GRANITIC GNEISS

Granitic gneiss crops out in the southwestern part of the map area where it forms Whiteface Mountain, one of the highest peaks of the Los Pinos Mountains (Plate I). Outcrops are continuous only along the top of the mountain whereas the steep sides are largely covered with talus. Some exposures crop out in arroyos at the base of the mountain. The granitic gneiss exposed in the map area is the northernmost end of the unit mapped and named the Los Pinos Granite by Stark and Dapples (p.1136). Granitic gneiss comprises less than 10% of the map area. Granitic gneiss is bounded to the north, west and east by leptynolite. The leptynolite-granitic gneiss contact is very irregular; this characteristic is easily seen on the northernmost slope of Whiteface Mountain. This contact crosses the trend of the regional schistosity. The schistosity transects the contact and is present in the granitic gneiss, but is developed to a lesser degree than in leptynolite.

Granitic gneiss has a dull luster. Outcrops are either massive-looking with several wide-spaced cleavages (Fig.10), or very schistose. The two structural varieties occur in zones that trend parallel to the regional schistosity. Schistosity and gneissic layering are also parallel to the trend of regional schistosity. Schistosity is present at

least to a minor extent in all outcrops and wherever biotite is present it defines the schistosity. The rock is pink and red and gray; gray varieties occur where the quartz content is higher than the average and near lithologic contacts, especially along the western border. The rock weathers to a reddish-orange color. Granitic gneiss is generally fine-grained but quartz "eyes" as large as 8mm in diameter are common. The large quartz grains can be seen easily in most outcrops especially along the east-west trending portion of Whiteface Mountain. Many outcrops on top of the mountain are coated with "desert varnish". Epidote mineralization is localized along some thin fractures. Milky quartz veins, one to two inches wide, occur either randomly oriented or oriented parallel to schistosity, cleavage or joints. Vugs, lined with subhedral to euhedral quartz crystals or empty, are common. Empty vugs are more common and are generally elongate parallel to schistosity and gneissic layering.

The average composition of granitic gneiss is 60% feldspar, 34% quartz and 5% biotite. Of the feldspar 20% is plagioclase, generally albite or oligoclase, 15% is alkali feldspar as microcline or more rarely orthoclase(?), and 25% is microcline perthite. Plagioclase and alkali feldspar show alteration to white mica in some thinsections. Alkali feldspar is generally altered to a greater degree than plagioclase. Minor constituents include almandine

garnet, zoisite, magnetite, chlorite and rarely muscovite. Accessories are specular hematite, apatite, zircon, calcite and sphene. A minute amount of antigorite is present, probably altered from chlorite (?).

Intergrowths of quartz and feldspar, the latter commonly microcline perthite or microcline, are prominent microscopic textures. Thinsections consist of 20% to 80% intergrowths and average 50%. Many styles of intergrowths are represented in the granitic gneiss including graphic, symplektic and myrmekitic (Fig. 11, 12, & 13); graphic is the most common. The symplektite and myrmekite border or radiate from large feldspar or quartz grains. Individual intergrowth areas commonly attain diameters of 6mm.

Flow cleavage is marked by the parallel orientation of light brown to dark reddish brown biotite flakes 0.1mm to 0.3mm long in a granoblastic matrix of fine-grained quartz and feldspar. Fine-grained elongate areas of quartz and feldspar, and feather-shaped quartz-feldspar intergrowths are parallel to the cleavage in the rock; they apparently lie in the cleavage planes or include them. In one slide (# 681) minor amounts of xenomorphic zoisite lie in the cleavage planes and thus mark them. Where flow cleavage is absent, a moderate to widely-spaced fracture cleavage is present. Flow cleavage commonly envelops large (1mm to 6mm) xenomorphic quartz and feldspar grains and phacoids of fine-grained quartz and feldspar. Mylonitic textures

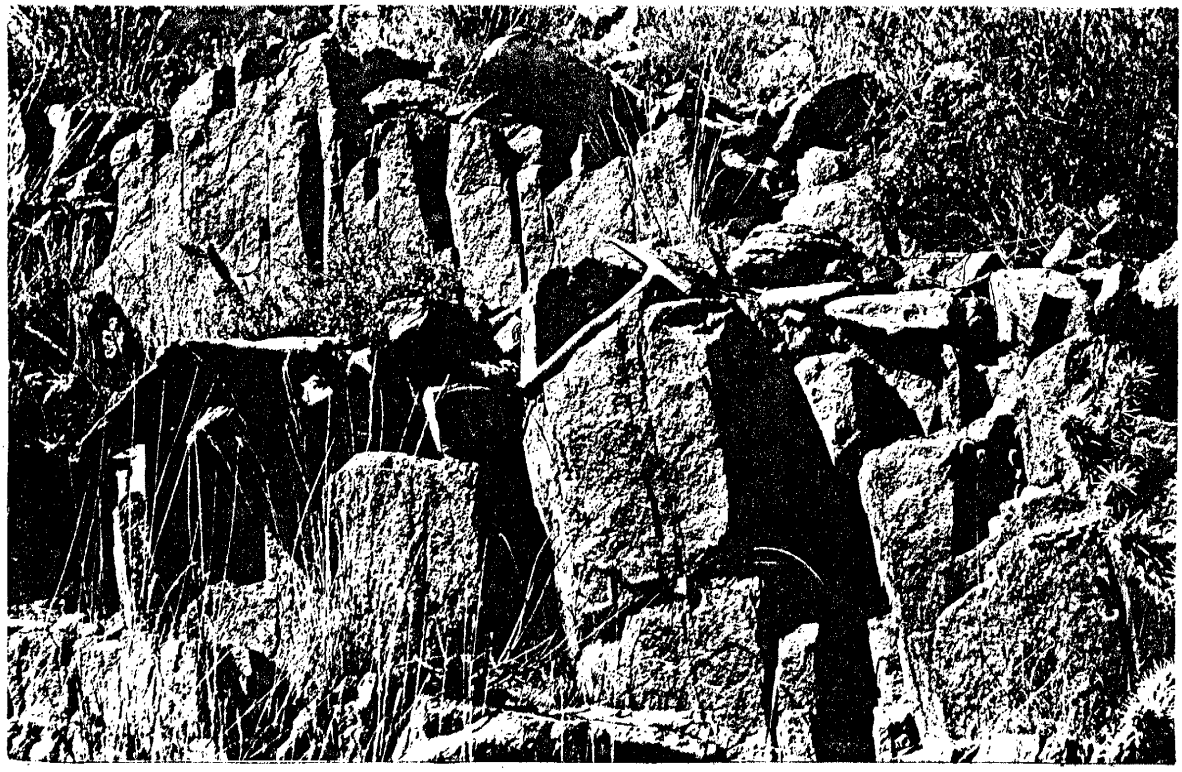

Figure 10. Granitic gneiss outcrop showing wide-spaced cleavage (perpendicular to plane of photo) cut by joints and a later cleavage (in the plane of the photo).

Figure 11. Graphic intergrowth of quartz and feldspar bordering a feldspar grain (X 160; X-nicols).

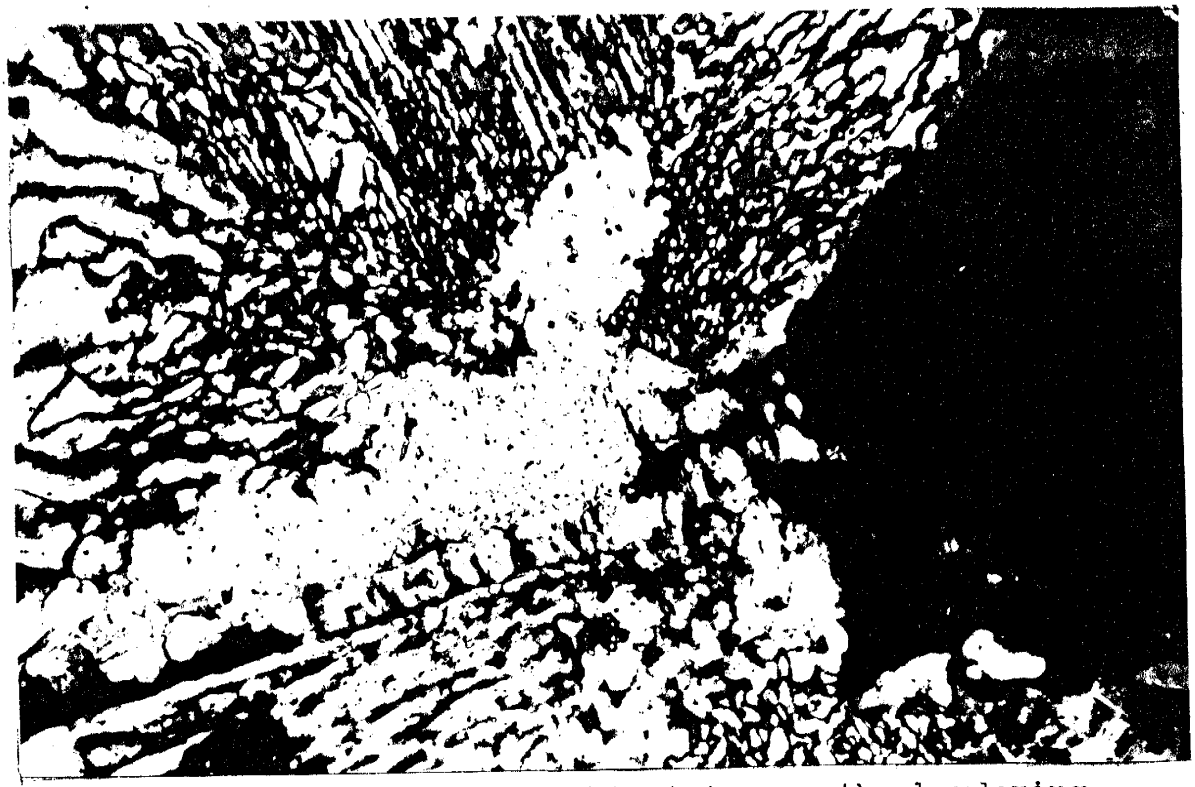

Figure 12. Myrmekitic and graphic intergrowths bordering quartz and feldspar grains. (X 450; X-nicols)

Figure 13. Odd-shaped quartz-microcline perthite intergrowth in granitic gneiss (X 160; X-nicols).

include large, rounded to sub-rounded quartz grains that exhibit sutured or uneven grain boundaries and undulatory extinction; subhedral and angular plagioclase grains show sheared areas and bent twin lamellae. Quartz-feldspar intergrowths are unaffected by (not cut by) flow cleavage, fracture cleavage and mylonitization. The only structural feature that affects the intergrowths to any extent is an incipient fracture cleavage that cuts all minerals and is oriented about 60^{o} to 90^{o} to the northeast trending prominent flow and fracture cleavage. Poikiloblastic texture is shown by large quartz and feldspar grains that include biotite, muscovite and accessory minerals. Large quartz grains commonly contain planes of minute inclusions which are colorless and have high relief. Anastomosing veinlets of fine-grained material, especially quartz, are present in most thinsections.

Irregular patches and veinlets of milky quartz and pink alkali feldspar occur throughout the granitic gneiss. The feldspar content of these masses is higher in this unit than in all others. Some veinlets contain as much as 35% feldspar whereas the veinlets in other units rarely contain more than 20% feldspar.

Radiogenic dates on two samples of granitic rock five miles south of the map area have produced anomalous results. One sample provided a date of 1400 ± 40 my which is in accordance with the other Precambrian granitic rocks exposed

in New Mexico. However, the other sample provided a date of 900 ± 40 my (personal communication with Dr. J. Wasserburg, 1966). Although the samples that have been dated are similar in composition to the granitic gneiss of the map area, the two rocks are very different texturally. The dated rocks are much coarser-grained than the granitic gneiss, and contain no recognizable quartz-feldspar intergrowths, whereas the granitic gneiss contains up to 80% intergrowths. The dated rocks contain none of the metamorphic textures that the granitic gneiss contains, e.g. flow and fracture cleavage, mortar texture, sutured quartz grain boundaries, and bent plagioclase twin lamellae. There exists the possibility that the dated rocks represent an igneous event younger than the youngest metamorphic event that has affected granitic gneiss in the map area. Another possibility is that the dated rocks were sampled from more massive zones of the granitic gneiss. Perhaps the different age dates reflect an anomalous isotope modification during one or more of the complex deformations that have affected the rocks in the map area. Or perhaps one of the rocks has been metamorphosed (thermally or regionally) and the other rock has not undergone metamorphism.

*

HORNBLENDE-CHLORITE SCHIST

Hornblende-chlorite schist consists of hornblende, chlorite, epidote, ± quartz, and ± plagioclase. It occurs

* See footnote following page.

as interlayers within parts of the leptynolite and muscovitic quartzite belts (Fig. 14). The thickness of individual layers ranges from a few inches to approximately 150 feet, but most layers are from five to 40 feet thick. Layers are most abundant in the central and eastern parts of the leptynolite belt and in the western part of the central muscovitic quartzite belt. Rare discontinuous layers crop out in the eastern belt of muscovitic quartzite. One or two layers crop out within the granitic gneiss exposure. Outcrops are generally poor, discontinuous, and form local topographic lows between highs produced by the surrounding rocks. Contacts are rarely well-exposed.

Hornblende-chlorite schist is most commonly dark green to black, but some have a mottled green and white coloring. Color is generally a function of plagioclase content: the higher the percentage of plagioclase, the lighter the color. The green color of the rocks is due to the presence of hornblende, chlorite and epidote. The rock usually has a dull luster but some samples possess a silky luster due to

*A note of explanation is required since the rocks of this unit were not mapped in the field. Although most outcrops of hornblende-chlorite schist are too small for the scale of the map, there are some that could have been mapped. There are several reasons why these rocks have not been mapped, the most important of which is the lack of time. The relatively poor outcrops of this rock and its relatively unexposed contacts necessitate the expenditure of much time in order to trace out approximate contacts. The decision was made by the author to collect all available pertinent data concerning this rock and to forego mapping it in order to spend the time collecting other more valuable data.

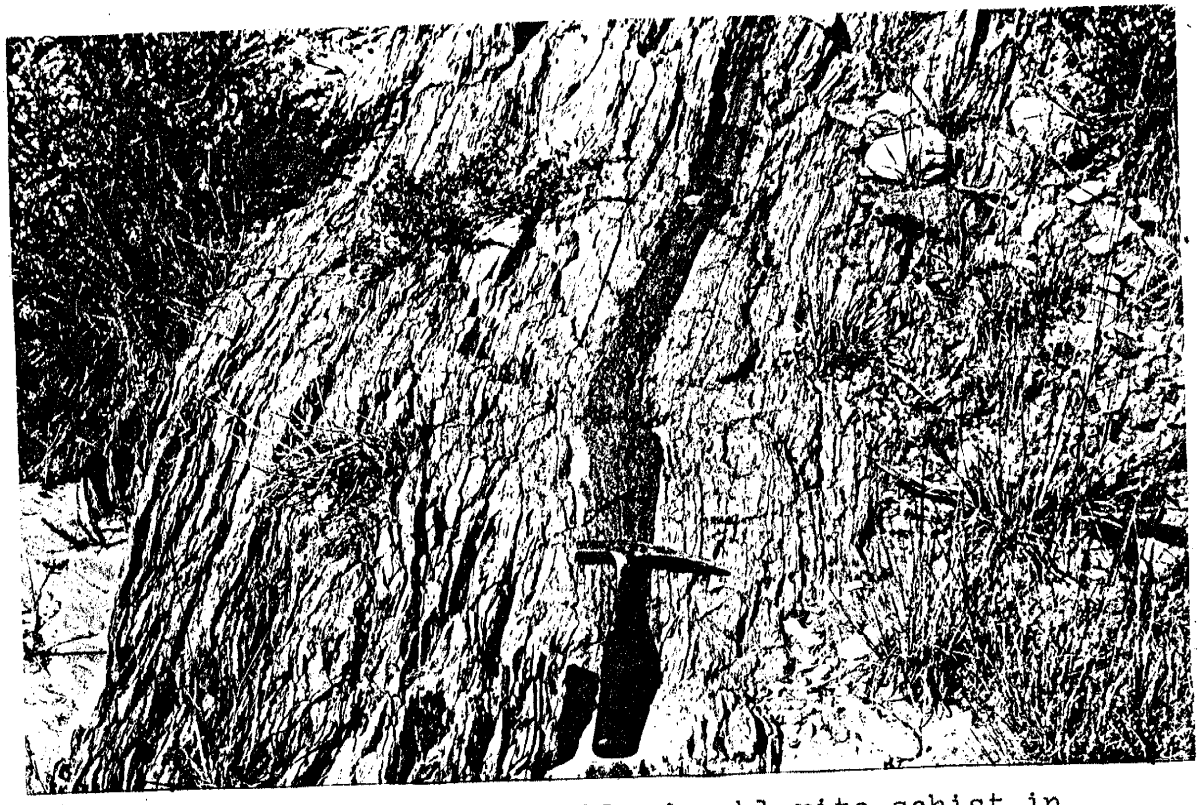

Figure 14. Interlayer of hornblende-chlorite schist in leptynolite.

a high percentage of chlorite aligned in the plane of schistosity. This unit is generally very schistose, except for layers with a high percentage of epidote. Some outcrops, especially those in the central and western parts of the leptynolite belt, are so schistose and cleaved in two or three directions that they crumble when struck with a hammer. Schistosity in hornblende-chlorite schist is parallel to schistosity in adjacent rocks. Mineralogic and textural lineation is present in schistosity planes. Rare folds occur, especially in outcrops along the spurs near the northeast side of the granitic gneiss exposure.

Hornblende-chlorite schist is extremely variable in composition and is here divided into four major mineralogic varieties. They are listed below in decreasing order of abundance and with their average compositions:

(1) Hornblende-quartz-plagioclase-chlorite schist: 50% hornblende, 20% quartz, 14% plagioclase, 8% chlorite, 5% epidote, and 1% magnetite;

(2) hornblende-epidote-chlorite-quartz schist: 45% hornblende, 25% epidote, 15% chlorite, 12% quartz, and 2% magnetite;

(3) hornblende-epidote-chlorite-plagioclase schist: 60% hornblende, 20% epidote, 10% chlorite, 7% plagioclase, and 1% magnetite;

(4) epidosite: 75% epidote, 15% quartz, 7% chlorite, 1% magnetite, and 1% biotite.

plagioclase occurs as twinned and untwinned grains. Oligoclase, about An_{27}, is the most common plagioclase, but albite is also present. Calcite partially replaces plagioclase and is also present to a minor extent in the matrix of the rock. Accessory minerals common to all four varieties of this rock are zircon, sphene and hematite; muscovite and biotite occur in a few samples. Excluding the epidosite the varieties of hornblende-chlorite schist are similar in texture and grain size and are described together.

Mica flakes, ranging from 0.05mm to 0.2mm in diameter, mark the prominent lepidoblastic texture. Chlorite is developed in two orientations, one defining the dominant flow cleavage, and another oriented at 90° to the flow cleavage and transected by it. A few decussate clots of chlorite are present and are transected and shredded by the dominant flow cleavage. Flow cleavage is mildly flexed by a later slip cleavage; this is most easily seen where chlorite is extensively developed. Some samples show nematoblastic hornblende idiomorphs 0.2mm to 2,5mm long and some smaller epidote prisms aligned within the flow cleavage planes. Hornblende most commonly forms radiating groups of prisms which either lie in or across the planes of schistosity. Hornblende crystals are generally zoned with light green centers and dark green edges. A few hornblende-chlorite schist samples show segregation layering of chlorite or biotite-rich schistose zones and fine-grained (0.05mm to

0.2mm) granoblastic quartz and feldspar-rich areas. Quartz forms small grains in the matrix and large grains with undulatory extinction. Flow cleavage usually envelops any large grains, but some minute micas that define the flow cleavage are enclosed within large optically continuous quartz grains. In one thinsection stringers of small quartz grains are arranged parallel to the dominant schistosity. Incipient fracture cleavage is approximately perpendicular to schistosity.

Epidosite forms boudins and irregular masses within the hornblende-chlorite schist layers. It is also common as pod-shaped masses in axial areas of folds. The composition of this rock is listed above. Epidosite does not generally exhibit schistosity and is vaguely granoblastic. Average grain diameter is approximately 0.1mm.

Thin fracture and vein fillings are commonly composed of small epidote grains. One to two millimeter wide fractures around the noses of folds are filled with epidote and are found in hornblende-chlorite schist located on spurs extending from the northeast corner of Whiteface Mountain. These epidote fillings have a one millimeter thick coating of pink potassium feldspar, verified by X-ray diffraction, and believed to be adularia.

METAMORPHISM

Precambrian rocks of the northern part of the Los Pinos

Mountains are polymetamorphic. At least three periods of deformation are recognized, with a thermal metamorphic period that occurs between the first two deformations. Retrograde metamorphism occurs either with or before the last deformational period, and after the thermal event.

There are a few general characteristics that most geologists use to distinguish the two main types of metamorphism, contact and regional. Contact metamorphism has generally been found to be somewhat local in extent, whereas regional metamorphism is usually large in areal extent. Contact metamorphism is generally related to some type of igneous intrusion; regional metamorphism is usually considered to have no obvious relation to igneous activity. Regionally metamorphosed rocks are generally believed to have formed by recrystallization associated with stress or shear movements; the resulting rock textures usually indicate that some kind of stress has been acting on the rock body. These textures include flow cleavage (schistosity), and slip and fracture cleavage. Contact metamorphic rocks are usually thought to have formed by simple recrystallization without stress. The resulting indicative texture is granoblastic or hornflesic, generally void of flow cleavage. Contact rocks have characteristic field relations; the rocks usually occur as aureoles which at least are more or less concentrically situated around an igneous body that is believed to have produced the metamorphism.

If the rocks in the northern part of the Los Pinos Mountains are to be classified as either contact or regional by the above criteria, they are regional. The bases necessary to differentiate the metamorphic history of the rocks of the map area are two: textural and petrologic features. On the basis of these two types of features the metamorphic history of the rocks of the northern part of the Los Pinos Mountains is divided into five major stages, some or all of which overlap to various extents. There are three periods consisting of rock movements ± recrystallization, which are called deformations, e.g. first, second and third deformation, and two periods in which recrystallization is the only recognizable feature. The writer considers it important to point out here that cataclastic textures are everywhere present on microscopic and mesoscopic scales in the northern part of the Los Pinos Mountains. These textures give some indication as to the type and style of metamorphism that the rocks have undergone.

First Deformation

The first deformation is characterized by intense componental slip movement accompanied by recrystallization. Slip movements resulted in the formation of shear folds and isoclinal flow folds with compositional layering (original bedding?) as the folded element. Axial plane cleavage to

the folds is a penetrative and pervasive schistosity that is defined by minute mica flakes with a high degree of preferred orientation. The schistosity has a consistent strike of N 20° - 30° E and produces the prominent layered effect that is present everywhere in the map area. The rocks are recrystallized and the resulting matrix mineral phases include much quartz, moderate amounts of muscovite and feldspar (plagioclase, microcline, microcline perthite, and rarely orthoclase), and biotite, chlorite, zoisite, epidote, hornblende, garnet and kyanite. Relict cataclastic textures, such as very close-spaced fracture cleavage, undulatory extinction and uneven or sutured grain boundaries, are commonly recognizable even though the rocks are recrystallized.

Thermal Metamorphism

Thermal metamorphism generally results in chemical and/or mineralogical reconstitution of rocks or parts of rocks. Heat is the principal agent of this type of metamorphism and stresses or directional movements are generally well-formed and commonly have well defined crystal outlines.

In the map area thermal metamorphism has resulted in the recrystallization of large biotite and chlorite flakes from available material in different rock types. Green to brown biotite, which is generally considered the low grade (grade here refers to the degree of intensity of metamorphism, specifically within different subfacies of the greenschist

facies) biotite (Tilley, 1926, p.34), occurs in feldspathic quartz-muscovite-biotite schist, granitic gneiss amd to a lesser extent in muscovitic quartzite and leptynolite. Components necessary for the recrystallization of biotite are all present in the rocks: K_2O and Al_2O_3 could have been derived from feldspar or muscovite and (Fe,Mg)O could have been derived from accessory minerals. SiO_2 is in excess in the rocks and is thus easily available for the formation of the biotite.

Thermal biotite generally occurs as grains similar in size to the rock's matrix grain size, but in the feldspathic quartz-muscovite-biotite schist the biotite occurs as large, ragged porphyroblasts. In all samples the thermal biotite is oriented at a high angle to micas that define the first deformation flow cleavage. In the rocks of the map area thermal biotite is always cut by second deformation cleavage. The best example of the cross-cutting relationship between thermal biotite and cleavage is seen in the thinsection of a sample taken from an outcrop of feldspathic quartz-muscovite-biotite schist located 1/2 mile S 20° W of Goat Ranch (see Plate Ia, sample #333). Figures 15a and 15b show large ragged biotite porphyroblasts in which are included grains that define first deformation flow cleavage; the biotite grains are bent and sheared by second deformation cleavage.

Chlorite that shows a brownish violet interference

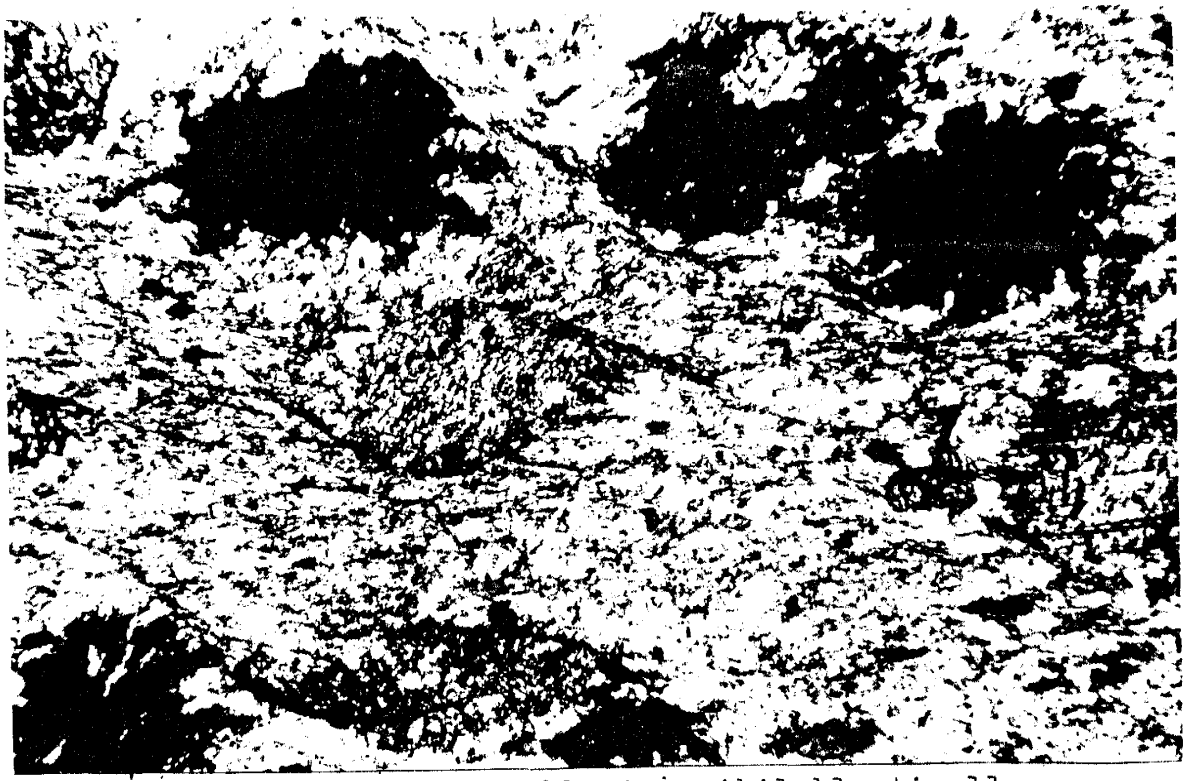

Figure 15a. Biotite porphyroblasts poikiloblastically including grains that define first defromation flow cleavage; biotite grains are bent and sheared by second deformation cleavage. (X160).

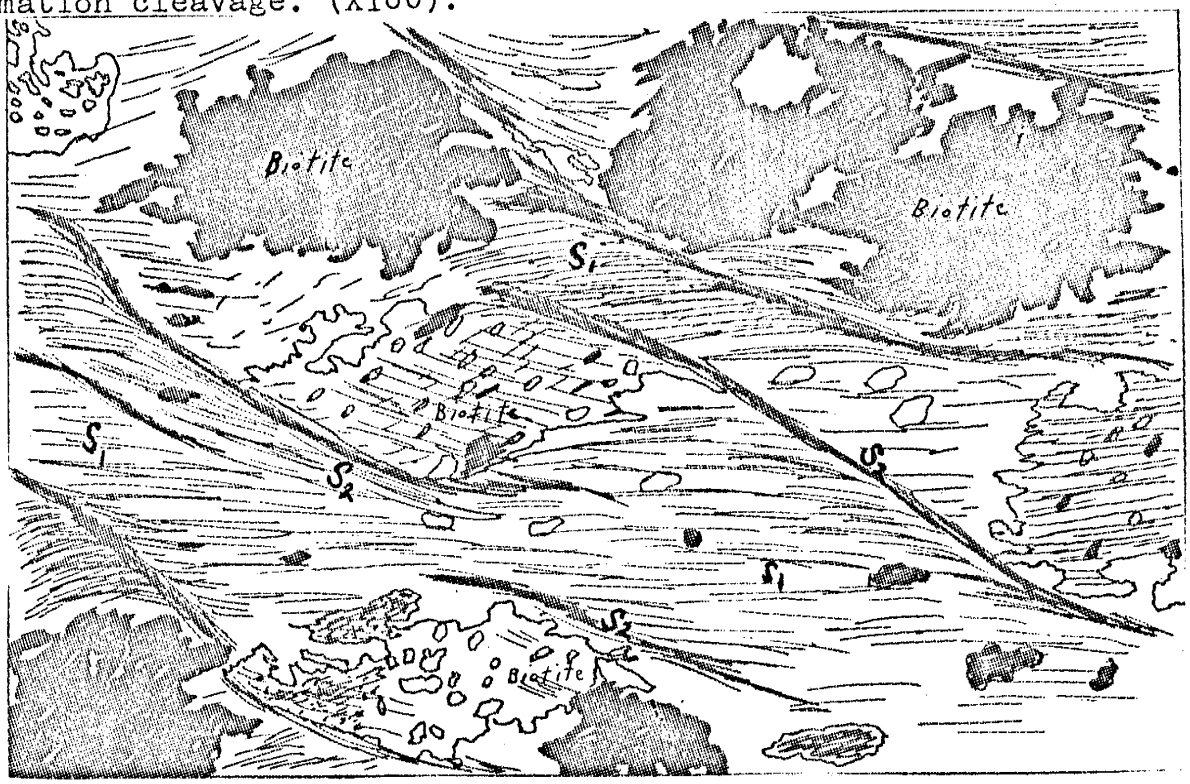

Figure 15b. Sketch of Fig. 15a indicating structural elements; all large grains are biotite.

color is generally considered high grade chlorite. This type of chlorite occurs in hornblende-chlorite schist. The chlorite could have formed from available material supplied by hornblende or minor amounts of micas and accessories; it could also have recrystallized from previously formed chlorite. Chlorite occurs as large porphyroblasts, aggregates of small grains, and as small matrix-sized grains. The grains are always oriented at some high angle to the micas that define first deformation flow cleavage. Second deformation cleavage transects thermal chlorite.

Almandine garnet is present as an accessory mineral in all rock units, but is abundant in one sample of feldspathic-quartz-muscovite-biotite schist (#333). The idiomorphic garnets have no preferred orientation. There are no rock textures that help determine the metamorphic period during which the garnets were formed.

Second Deformation

The second deformation is characterized by mechanical deformation with little or no recognizable accompanying recrystallization. Results of this deformation are slip cleavage and cleavage folds in schistose and phyllitic rocks, and fracture cleavage and flexural slip folds in the more competent quartz-rich rocks. Common microscopic textures include mortar texture, and sutured grain boundaries and undulatory extinction of quartz grains. These textures

are generally indicative of cataclasis. The presence of these textures also indicates that little or no recrystallization has taken place during or after the second deformation.

Retrograde Effect

The retrograde change of biotite to chlorite occurs in hornblende-chlorite schist and feldspathic quartz-muscovite-biotite schist. Mica flakes with biotite cores, narrow borders of chlorite, and irregular patches of chlorite within the biotite cores are textures that are interpreted as evidence of the retrograde effect. This change has affected the biotite grains produced during the first deformation and those produced by the thermal metamorphism. Planar structures of the last recognizable deformation cut grains that show the retrograde textures. Thus textural evidence places the retrograde effect somewhere between the thermal metamorphism and the last recognizable deformation.

Third Deformation - Dislocation Metamorphism

This deformation is considered as dislocation metamorphism because it has resulted only in the fracturing of rocks. No transport of material has been recognized. The product of this dislocation is non-penetrative, homogeneous and pervasive fracture cleavage. No recognizable chemical or mineralogic changes occur during this deformation.

METAMORPHIC FACIES CLASSIFICATION

Facies of regional metamorphism set forth by Turner and Verhoogen (1960, p. 531-560) are used here in an attempt to classify the metamorphic rocks of the northern part of the Los Pinos Mountains. Only those mineral assemblages that are products of regional metamorphism are considered under the facies concept, thus minerals that post-date the regional metamorphism and lack a preferred orientation are not considered here since they are not equilibrium phases of the regionally metamorphosed rocks (assuming the rocks are actually products of regional metamorphism).

The facies classification is applicable only to equilibrium assemblages. The structural criterion of equilibrium is a single movement picture with mutually intergrown minerals possessing a high degree of preferred orientation. The chemical criterion of equilibrium is Goldschmidt's mineralogic phase rule (the number of phases is equal to, or less than, the number of components). The mineral assemblages of all the rocks with the exception of hornblende-quartz-plagioclase-chlorite schist and hornblende-epidote-chlorite-plagioclase schist are equilibrium assemblages and are amenable to facies treatment. All of the assemblages exhibit a fabric characteristic of the first deformation. Although the exceptions noted above comply with the phase rule, some of the mineral phases are not expectable in common equilibrium assemblages. The association of chlorite and

oligoclase (in some samples the composition is An_{26}, but in others it is about An_{30}) is typical in hornblende-quartz-plagioclase -chlorite schist and hornblende-epidote-chlorite-plagioclase schist, but it is not expectable as an equilibrium assemblage since chlorite and oligoclase have generally been considered incompatible. It is necessary to point out here that expectable equilibrium assemblages are those that have been commonly found by geologists to be texturally and mineralogically at equilibrium. It is possible that the chlorite-oligoclase assemblage could be at equilibrium since recent experimental studies have shown that chlorite can exist at equilibrium at temperatures and pressures characteristic of the almandine-amphibolite facies. Thus chlorite is not restricted to environments typical of the greenschist facies, as has been previously believed.

The equilibrium assemblages of regional metamorphism that occur in the map area are shown in Table I. With the exception of the four mineralogic varieties of hornblende-chlorite schist, all the assemblages can be placed in either the greenschist facies or both the greenschist and almandine-amphibolite facies. Those assemblages that can be placed in both facies have minerals characteristic of both facies, but lack critical minerals of either facies.

Feldspathic quartz-muscovite-chlorite schist, feldspathic quartz-muscovite-biotite schist, and granitic gneiss are placed in the greenschist facies because of the presence

TABLE I

Equilibrium assemblages of regional metamorphism in the northern part of the Los Pinos Mountains

Rock unit	Equil. assemblage (+quartz) (critical minerals in caps)	Facies
Muscovitic quartzite	muscovite, (ALBITE, K-feldspar) (feldspathic varient in parentheses)	greenschist or alm.-amphib. (greenschist)
feld. qtz-musc-chlor. schist	ALBITE-K-feldspar-muscovite CHLORITE	greenschist, chlorite subf.
feld. qtz-musc-biot. schist	ALBITE-BIOTITE-K-feldspar-muscovite	greenschist, biotite subf.
leptynolite	ALBITE-CHLORITE-BIOTITE-muscovite-microcline	greenschist, biot. & chlor. subfacies
hbld-chlor-qtz-plag schist	hbld-CHLORITE-OLIGOCLASE-perthite	NO ASSIGNMENT
hbld-epidote-chlor-qtz sch.	hbld-epidote-chlorite	greenschist or alm.-amphib.
epidosite	epidote-chlorite	greenschist or alm.-amphib.
hbld-chlor-ep-plag schist	hbld-CHLORITE-OLIGOCLASE-epidote	NO ASSIGNMENT
granitic gneiss	ALBITE-perthite-microcline-BIOTITE-ALMANDINE	greenschist, biotite or alm. subfacies

of albite and either biotite or chlorite. Feldspathic quartz-muscovite-chlorite schist is representative of the chlorite subfacies, feldspathic quartz-muscovite-biotite schist is placed in the biotite subfacies, and granitic gneiss is placed in the biotite-almandine subfacies. The largest part of the muscovitic quartzite exposure does not contain plagioclase, thus its equilibrium assemblage fits equally well in both the greenschist and almandine-amphibolite facies. The presence of albite in the feldspathic phase of muscovitic quartzite enables this rock phase to be placed in the greenschist facies. Leptynolite belongs in the greenschist facies, but the rock has minerals characteristic of both the biotite and chlorite subfacies.

Attempting to fit the hornblende-chlorite schists into the regional facies classification presents a few problems. Chlorite is intimately intergrown with hornblende in all of those schists except the epidosite, in which chlorite occurs with epidote. The presence of chlorite generally warrants classification in the greenschist facies. However, in the hornblende-quartz-plagioclase-chlorite schist and hornblende-epidote-chlorite-plagipclase schist, chlorite occurs in the presence of oligoclase, which is characteristic of the almandine-amphibolite facies. This problem is discussed by Bingler (1965, p.46-47) in relation to hornblende-chlorite schist occurring in La Madera quadrangle in New Mexico. In attempting to explain the chlorite

oligoclase (andesine) relationship he says:

> Abnormally high partial pressure of water would tend to extend the stability field of chlorite to the higher temperatures commensurate with the assumed P-T realm of the almandine-amphibolite facies (Nelson and Roy, 1958), but it would also facilitate the breakdown of andesine to albite plus epidote. The real problem lies in a lack of knowledge regarding the stability relations of chlorite under different partial pressures of water and FeO/MgO ratio. An alternative possibility is that biotite originally formed the matrix mica, and that subsequent removal of K_2O has converted biotite to chlorite.

Another problem which is encountered in the facies classification of the hornblende-chlorite schists is the validity of the identification of hornblende. Hornblende has been identified by optical methods, but hornblende and actinolite are indistinguishable optically. If the amphibole is actually actinolite, the equilibrium assemblages of the rocks in question would fit the greenschist facies as indicated by the actinolite-chlorite association. However, the presence of oligoclase still indicates the almandine-amphibolite facies. It is evident that the hornblende-chlorite schists of the northern part of the Los Pinos Mountains do not fit into any of the regional metamorphic facies as they are presently accepted.

PARENT ROCKS

Attempts to suggest origins for the Precambrian rocks of the map area are complicated by the complex polymetamorphic nature of the rocks. There is not much positive

evidence concerning the origin of these rocks and the suggestions put forth here are at least partly speculative.

Muscovitic quartzite probably represents a metamorphosed quartz sandstone. The presence of moderate amounts of muscovite could represent original presence of potassium alumino-silicate minerals. The feldspathic varient of muscovitic quartzite can either be explained as an originally arkosic varient of quartz sandstone, or as a result of the introduction of K_2O and Na_2O into part of the muscovitic quartzite. There is no good evidence for potassium and sodium metasomatism in the map area, and the simplest explanation, an original arkosic varient, seems to be the best explanation.

Feldspathic quartz-muscovite-chlorite and feldspathic quartz-muscovite-biotite schist and phyllite are probably derived from impure (pelitic ?) sandy shales or mudstones. The presence of a high percentage of muscovite probably indicates the original presence of clay minerals; the quartz represents the original sandy material of the rock. Feldspar probably denotes original impure material or recrystallized original feldspar.

As the name implies, granitic gneiss approaches granite in composition, but is very quartzose. Field relations of the mapped part of the granitic gneiss are inconclusive regarding the origin of this rock. It may represent an intrusive granite (Stark and Dapples, p.1136-1138)

some other plutonic rock of similar composition that as been polymetamorphosed. Granitic gneiss could also epresent polymetamorphosed granitized sediments.

Hornblende-chlorite schists are called basic schists y Stark and Dapples (p.1135-1136) who believed that the ocks were derived from basic igneous rocks. There are wo generally accepted origins for hornblende-chlorite chist or amphibolite: basic igneous rocks, and impure alcareous or dolomitic sediments. Usually if the meta- orphic rock has approximately equal amounts of plagioclase nd hornblende, the rock is considered to have been derived rom a basic igneous rock (Williams, Turner, Gilbert, 1954, p.240-243). Where the percentage of hornblende is igh relative to the percentage of plagioclase present in the rock, the original rock is considered to be an impure calcareous or dolomitic sediment (Williams, Turner, Gilbert, p.240-243). It seems logical that metamorphic rocks that are derived from impure calcareous or dolomitic sediments tend to vary more in composition than if they are derived from basic igneous rocks since the impure sediments have a more variable composition than basic igneous rocks. Hornblende-chlorite schists in the map area contain considerably more hornblende than plagioclase, and the schists also have extremely variable compositions. These two character- istics suggest a sedimentary rather than an igneous origin. If a sedimentary origin is accepted, then the presence of

moderate amounts of quartz in the hornblende-chlorite schists suggests that the sediments were not only calcareous or dolomitic, but also siliceous. Field investigation has not revealed any evidence concerning the pre-metamorphic nature of the hornblende-chlorite schist.

The rock named leptynolite in this report has been identified as rhyolite by Stark and Dapples (p. 1134). Supposedly the same rock is exposed in the South Manzano Mountains and has been called metarhyolite by Stark (1956, p.11); the rock has also been called metarhyolite by Reiche (1949, p.1191) in the North Manzano Mountains. Field relations and petrographic data are cited by these authors as evidence for the volcanic origin of leptynolite. The flow lines and chilled borders mentioned by Stark and Dapples (p.1135) have not been seen, even in detailed investigations. The presence of large feldspar and quartz "phenocrysts" (p. 1135) and a fine-grained matrix of quartz and feldspar have been used as criteria for identification as rhyolite. However, as mentioned in the section describing muscovitic quartzite, the westernmost exposures of muscovitic quartzite contain large quartz and feldspar grains, similar to those in leptynolite. This indicates the possibility of simple recrystallization from parent material as the mode of origin for the large grains. The large grains are therefore not necessarily relict. British petrologists believe that feldspar "phenocrysts" could remain almost intact through polymetamorphism (Brown, 1965, p.348), but

if the large grains in leptynolite are relict, it is geologically inconsistent for only one rock unit of an equally metamorphosed series to retain relicts. The wide range in composition of the large feldspar grains is not a very common characteristic of volcanic rocks. The presence of large quartz grains in this rock unit is another problem. Many geologists argue that these quartz grains are bipyramids, indicating an original volcanic rock. There is no petrographic evidence that indicates a bi-pyramidal nature of the quartz grains. Another criterion which supposedly suggests a volcanic origin for leptynolite is that rock is a thick, continuous series of flows. The presence of feldspathic quartz-muscovite-chlorite and feldspathic quartz-muscovite-biotite schist and phyllite interlayers in leptynolite indicates that the rock unit is not one continuous unit. An alternate hypothesis for the origin of leptynolite is that the parent rock is an arkosic sandstone which has been finely granulated during meta-morphism. The large quartz and feldspar grains could be relicts in the sense that they have not been crushed and granulated. Large feldspar grains could have recrystallized from material in the rock's matrix, or they could have been recrystallized from material introduced during the thermal metamorphic period. Leptynolite resembles the phyllonites described by Knopf (1931, p.1-27). An origin from previously metamorphosed granulites is a possibility if the leptynolite

is a phyllonite. The structure and textures common to phyllonites are present in the leptynolite of the northern Los Pinos Mountains.

Structural Geology

INTRODUCTION

Detailed structural investigation of the Precambrian metamorphic rocks of the northern part of the Los Pinos Mountains reveals multiple fold systems whose superposition suggest at least three separate and temporally distinct deformational periods. Multiple fold systems form by either of two methods: a very complex or multipe stress field operating at one time, or several stress fields operating at different times and superposed on each other. Criteria for the latter method are systematic but different orientations for each structural system, sequential age relationships of fold elements and characteristic style of deformation associated with each structural system (Freedman and others, 1964, p.622). The three structural patterns, including two fold systems, of the northern Los Pinos Mountains are separated on the basis of these criteria.

Structural study of the metamorphic rocks of the map area has produced the following results. First, planar structures such as flow cleavage and fracture cleavage are representative of three and possibly four deformations. Second, prominent lineations were produced by three defor-

mations, but only two deformations have produced recognizable fold systems. Third, the areal distribution, style and orientation of individual folds have been determined for the two fold systems. Fourth, the structural effects of the superposition of successive stages of deformation have been determined. And fifth, a relative time sequence has been established for the superposed deformations.

In order to avoid confusion and limit verbosity in the following sections a list of the definitions of structural terms and symbols used in this thesis is included in the glossary.

PRE-FIRST DEFORMATION

S_o is defined by the parallel and semi-parallel arrangement of minute mica flakes. It has been identified only on a microscopic scale in a few thinsections, and thus its attitude in the field has not been recorded. Planes of S_o are generally very vague and lie between planes of S_1 where the latter are spaced widely enough to permit this observation. S_o intersects S_1 at angles ranging from 40^o to 70^o and produces mineralogic L_1 on S_1 planes. In one or two samples S_o planes are slightly sigmoidal, suggesting that S_1 in these particular samples is a slip cleavage. S_o belongs to no recognizable deformation and therefore cannot be shown to be of tectonic origin. It is possible that S_o represents primary stratification (bedding?).

FIRST DEFORMATION

Regional metamorphism of the Precambrian rocks of the northern Los Pinos Mountains has resulted in the most profoundly developed structural features in the map area. Intense shearing has produced complete transpostion of primary compositional layering (bedding ?), and homogeneous and penetrative cleavage. D_1 has produced F_1 folds but the shearing and transposition of compositional layering has been so intense that almost all F_1 folds have been destroyed.

Microscopic Structures

Most thinsections contain microscopic evidence of S_1 as flow cleavage in micaceous rocks, as fracture cleavage in rocks deficient in micas, and as slip cleavage in rocks that show S_1 transecting sigmoidal S_o planes. One F_1 flow fold has been identified (Fig. 16). The fold is marked by a 0.3mm thick layer of quartz grains within the mica, quartz and feldspar-rich matrix of a leptynolite sample. This F_1 fold has S_1 as axial plane cleavage.

In feldspathic quartz-muscovite-chlorite and feldspathic quartz-muscovite-biotite schist, S_1 flow cleavage is defined by the parallel and semi-parallel orientation of minute mica flakes either in segregated layers or evenly distributed throughout the rock's matrix. Minute mica flakes with a high degree of preferred orientation are generally evenly distributed throughout the matrix of leptynolite and muscovitic quartzite. In biotite-rich phases of

granitic gneiss, biotite grains are commonly larger than in other rock units and occur in layers parallel to S_1. S_1 flow cleavage in hornblende-chlorite schist is marked by the preferred orientation of chlorite flakes and hornblende prisms.

S_1 fracture cleavage in biotite-poor phases of granitic gneiss occurs as variably-spaced fractures which transect most grains; only a few quartz-feldspar intergrowths are cut by the fracture cleavage. S_1 fracture cleavage planes in muscovitic quartzite are very close-spaced and cut all grains.

Mesoscopic Structures

Folds

Mesoscopic structures are by far the most obvious features of D_1. F_1 folds are not common due to intense shearing and transposition during D_1 as previously explained. Twelve F_1 isoclinal flow or cleavage folds have been measured in the field. All have S_1 fracture cleavage or flow cleavage as axial plane cleavage. The axes of F_1 folds generally bear N 65° W and plunge 50° to 70° west; this trend ranges from N 10° E, 20° NE to N 85° W, 85° NW as can be seen on Plate II which is a lower hemisphere equal area projection of F_1 axes. Axial planes consistently strike N 20-25° E and dip 40-70° NW. The folded element in F_1 folds in muscovitic quartzite is usually hematite and magnetite-

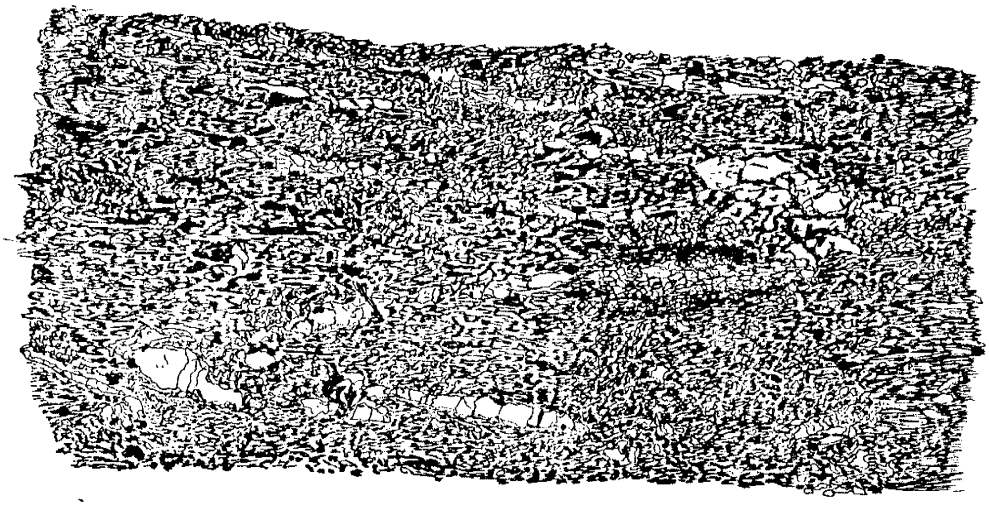

Figure 16. Projection drawing of F_1 fold; folded element is a layer of quartz grains in quartz-feldspar-mica matrix of leptynolite. Schistosity is axial plane cleavage to the fold (X 20).

Figure 17. Isoclinal F_1 flow fold of a hematite and magnetite-rich layer in muscovitic quartzite; axial plane cleavage is S_1.

rich layers (Fig. 17-18), but a few exposures show folded quartz layers. In feldspathic quartz-muscovite-chlorite and feldspathic quartz-muscovite-biotite schist the folded element is either black layers rich in magnetite, hematite or biotite (Fig. 19) or layers alternately rich and poor in iron-bearing phases (Fig. 20-21). F_1 folds in leptynolite commonly fold white and pink feldspar-rich layers. The folded layers in all the rocks are generally 1/16 inch to 1 1/2 inches thick. No F_1 folds were identified in hornblende-chlorite schist and granitic gneiss. Although most F_1 folds have an isoclinal flow or cleavage style, some are mild flexure or crinkle folds (Fig. 20). One outcrop of muscovitic quartzite shows ptygmatic folding of thin iron-rich layers. Many F_1 folds have sheared out axial planes (Fig. 18) eliminating or juxtaposing one of the fold limbs and leaving visible one arcuate lime resembling a cross bed. Many of these arcuate limbs can be identified as folds and not cross beds due to their folded nature which is not characteristic of cross beds. Although only twelve F_1 folds have been measured in the field, many more are present but their measurement is not possible due to the physical character of the outcrops. Folded elements have been identified on many horizontal joint planes, but traces of fold axes have not been found on other planar surfaces, thus only very rough estimates of the trend of fold axes have been made.

Figure 18. F_1 shear fold in muscovitic quartzite with sheared out axial plane.

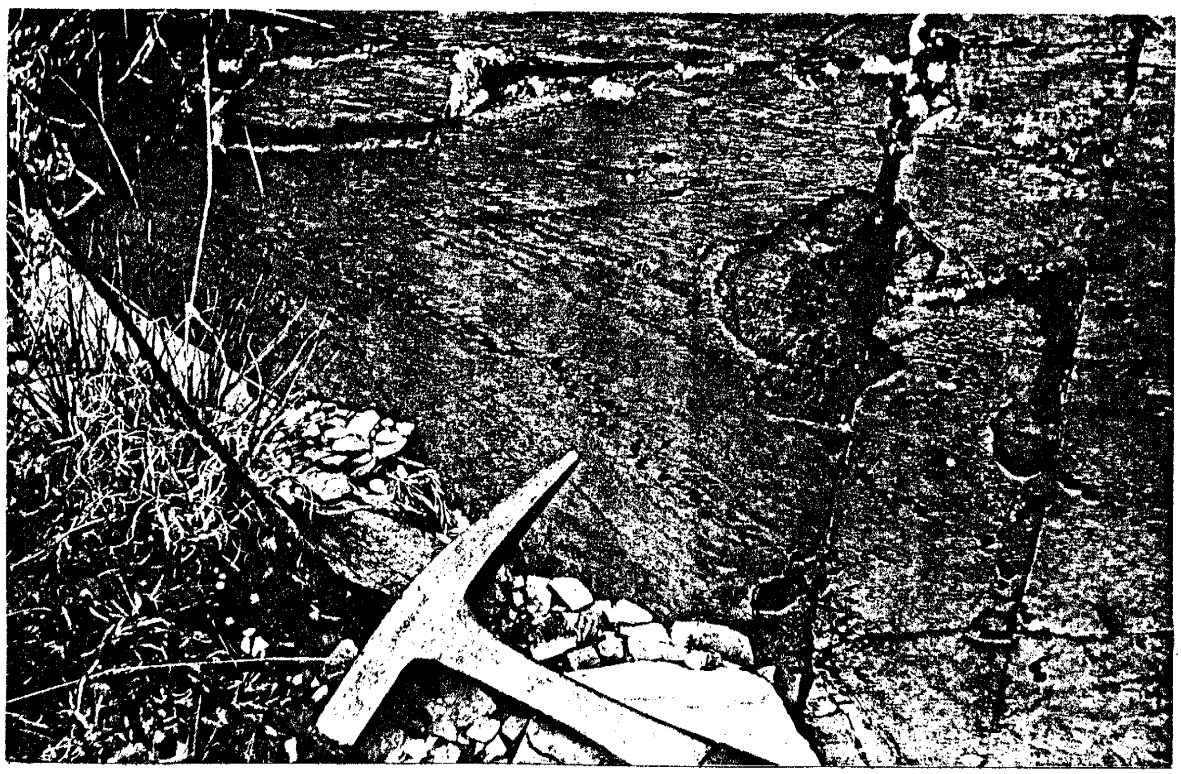

Figure 19. Biotite layers in feldspathic quartz-muscovite-biotite schist forming F_1 shear folds with S_1 flow cleavage as axial plane cleavage.

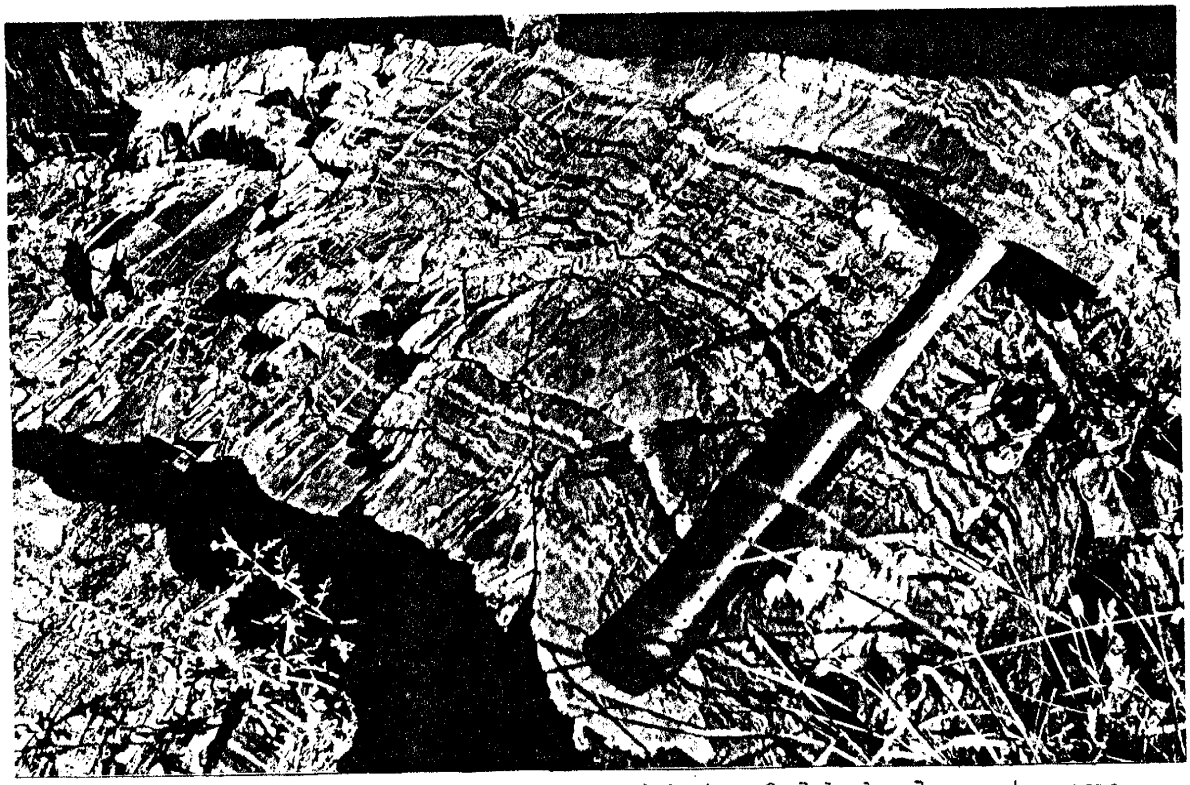

Figure 20. F_1 crinkle folds in schist; folded elements are alternating iron-rich and iron-poor layers. Axial plane cleavage is S_1 flow cleavage.

Figure 21. F_1 folds in schist; light layers are quartz-rich. S_1 axial plane cleavage cuts fold limbs and nose.

Planar Structures

Homogeneous and penetrative S_1 is flow cleavage in all lithologic units except muscovitic quartzite and biotite-poor phases of granitic gneiss where S_1 is fracture cleavage. S_1 planes and parallel compositional layers produce the prominent layering that is present in every outcrop in the northern Los Pinos Mountains. S_1 generally strikes N 20°-30° E and dips 40°-70° NW. A lower hemisphere equal area projection of S_1 (Plate III) illustrates the variation in trend of this planar element. Since S_1 is parallel to F_1 axial planes, S_1 can everywhere be considered axial plane cleavage to F_1 (this can be seen in many of the photos cited in the F_1 fold descriptions). S_1 therefore does not represent original stratification, although it may parallel bedding because of the isoclinal nature of F_1.

There are several structures that resemble primary stratification. Grain size alternately changes from coarse-grained to fine-grained in zones that are consistent in thickness and are parallel to S_1. This textural layering is found in muscovitic quartzite and less commonly in leptynolite. Coarse-grained quartz stringers in a fine-grained matrix are parallel to S_1 in leptynolite.

The granitic gneiss contact cuts across the regional trend of S_1. S_1 is parallel to all other map unit contacts. Although S_1 is present in granitic gneiss, the planes of S_1 are not as close-spaced in this unit as in the other units.

S_1 planes in granitic gneiss occur in zones in which the planes are alternately close-spaced and wide-spaced. Even in the close-spaced cleavage zones, S_1 planes are rarely as penetrative as they are in the other rock units.

Quartz layers

Layers and veinlike masses of milky quartz occur in all the rock units. They are usually parallel to S_1, but in places they transect planes of S_1 or lie in joint planes. Microscopically the quartzose areas show extreme cataclastic textures plus the development of two fracture cleavages, one coincident with S_1 and the other (S_3) oriented at about 90^{o} to S_1. The thickness of the layers ranges from less than 1/4 inch to eight feet. Approximately in the southern half of the map area pinkish-orange, coarse-grained K-feldspar appears as a phase with the milky quartz in the layers and veins. The percentage of K-feldspar in the layers increases toward the southwestern corner of the map area, i.e. toward exposed granitic gneiss. Frequency of occurrence of layers and veins also increases toward the southwestern corner of the map area. Layers and veins are very common in parts of the granitic gneiss exposure where individual veins and layers are one to two inches thick and occur only six to eight inches apart.

The textural and mineralogic nature of the quartz-feldspar layers and veins suggests an origin associated with

igneous activity, i.e. these layers and veins are pegmatitic and therefore could be associated with the granitic gneiss as a last phase of igneous activity before metamorphism (this of course assumes an igneous origin for granitic gneiss). Layers and veins composed only of quartz could have the same origin as the feldspar-quartz varieties. Quartz layers and veins are generally found at a greater distance from the granitic gneiss than the feldspar-quartz variety; this could indicate that the late stage "pegmatitic" solutions simply became depleted in feldspathic components at great distances from the parent rock. Another possibility for the origin of the quartz masses is that silica was very mobile during one or more of the metamorphic periods, and siliceous solutions penetrated the map area forming layers and veins of milky quartz.

Spatial relations between the quartz and feldspar-quartz masses and the prominent structural features of the map area indicate that the layers and veins for the most part are associated with the first deformation. However, as indicated above, there is evidence that the quartz masses are related to structural (?) events younger that the first deformation.

Linear Structures

D_1 has produced mineralogic and textural lineation. L_1 on S_1 planes. L_1 usually bears N 60°-85° W and plunges

50°-80° NW. Its range in trend can be seen on Plate IV, which is a point diagram of L_1 lineation. Where F_1 folds are present their axes are always parallel to L_1 which indicates that L_1 is a b-lineation. Three types of L_1 have been found. The first is F_1 fold axes. The second type is the trace of the intersection of S_o planes with S_1 planes. The micas that define S_1 flow cleavage have a semi-parallel nature. Two general mica orientations have a dihedral angle of 5°-10°. The two orientations together define S_1, but since the micas are actually at a small angle to S_1, they all intersect this S-plane. This intersection of S_1 planes with mica flakes produces the third and most common type of L_1. Some L_1 in hornblende-chlorite schist is produced by the parallel aligment of the long axes of hornblende needles. L_1 in granitic gneiss is marked by streaks of fine-grained quartz plus the intersection of biotite flakes with S_1.

Boudins

Boudins are linear structures and in the map area they generally lie in S_1 planes. The long axes of these boudins trend parallel to L_1. Boudins are commonly crumpled or flexed. Boudins in the map area usually consist of milky quartz, but some within hornblende-chlorite schist are epidote. Quartz boudins are usually the larger type. The cross sectional ratio (long axis : short axis) is measured

on outcrop surfaces generally 65^{o}-90^{o} to the axis of the boudin which plunges parallel to L_1. This average ratio is 2:1. The short cross sectional axes range from one inch to five feet. Long cross sectional axes generally range from one inch to ten feet, but a few are as long as 50 feet.

SECOND DEFORMATION

Cataclastic deformation, D_2, in the northern Los Pinos Mountains has produced a fold system, F_2, which is superposed on F_1. The orientation and style of F_1 and F_2 folds, and the relationships of folded elements, are considerably different. Although F_2 is the most obvious effect of D_2, well-formed S_2 slip cleavage and flow cleavage and L_2 textural lineation are both present.

Microscopic Structures

S_2 slip cleavage and flow cleavage is seen in many thinsections. S_2 slip cleavage is seen in many stages of formation in micaceous rocks (those containing 20% or more of micas). Where S_1 flow cleavage is mildly flexed by S_2, the distance between successive S_2 planes ranges from 0.2mm to 5mm. In samples that show S_1 more highly deformed by S_2 slip cleavage, S_1 planes are sigmoidally shaped between successive S_2 slip planes; S_2 planes at this stage of formation range from 0.3mm to 8mm apart. The last stage of formation of S_2 slip cleavage is exhibited in thinsections

that show close-spaced penetrative S_2 cleavage planes; in such samples all traces of S_1 flow cleavage have been obliterated by the intense formation of S_2 cleavage which in all respects is now flow cleavage. Figure 22 demonstrates three stages of formation of S_2 slip cleavage.

Mesoscopic Structures

Folds

The most obvious effect of D_2 in the map area is the folding of S_1 axial plane flow cleavage into mesoscopic F_2 folds. Ninety F_2 folds have been measured in the field. F_2 axial planes have no uniform strike, ranging from N 55° W to N 75° E, with a minor concentration at N 20°-25° E. F_2 axial planes dip much more uniformly, averaging about 55°-65° W-NW. F_2 axes bear N 25° E to S 15° W; the general northerly and westerly plunge is 35°-65° (see Plate V). F_2 folds have an irregular regional distribution, occurring mainly in elongate zones that parallel lithologic contacts (see Plate I). These folds are found in all map units except granitic gneiss. The best exposed F_2 folds occur along the crest of White Ridge and in feldspathic quartz-muscovite-chlorite and feldspathic quartz-muscovite-biotite schist layers within muscovitic quartzite (see Plate I). Only a few F_2 folds have been located east of White Ridge and within the leptynolite belt. Frequency of occurrence of F_2 folds increases from the leptynolite belt eastward to White Ridge and then abruptly diminishes. F_2 folds are

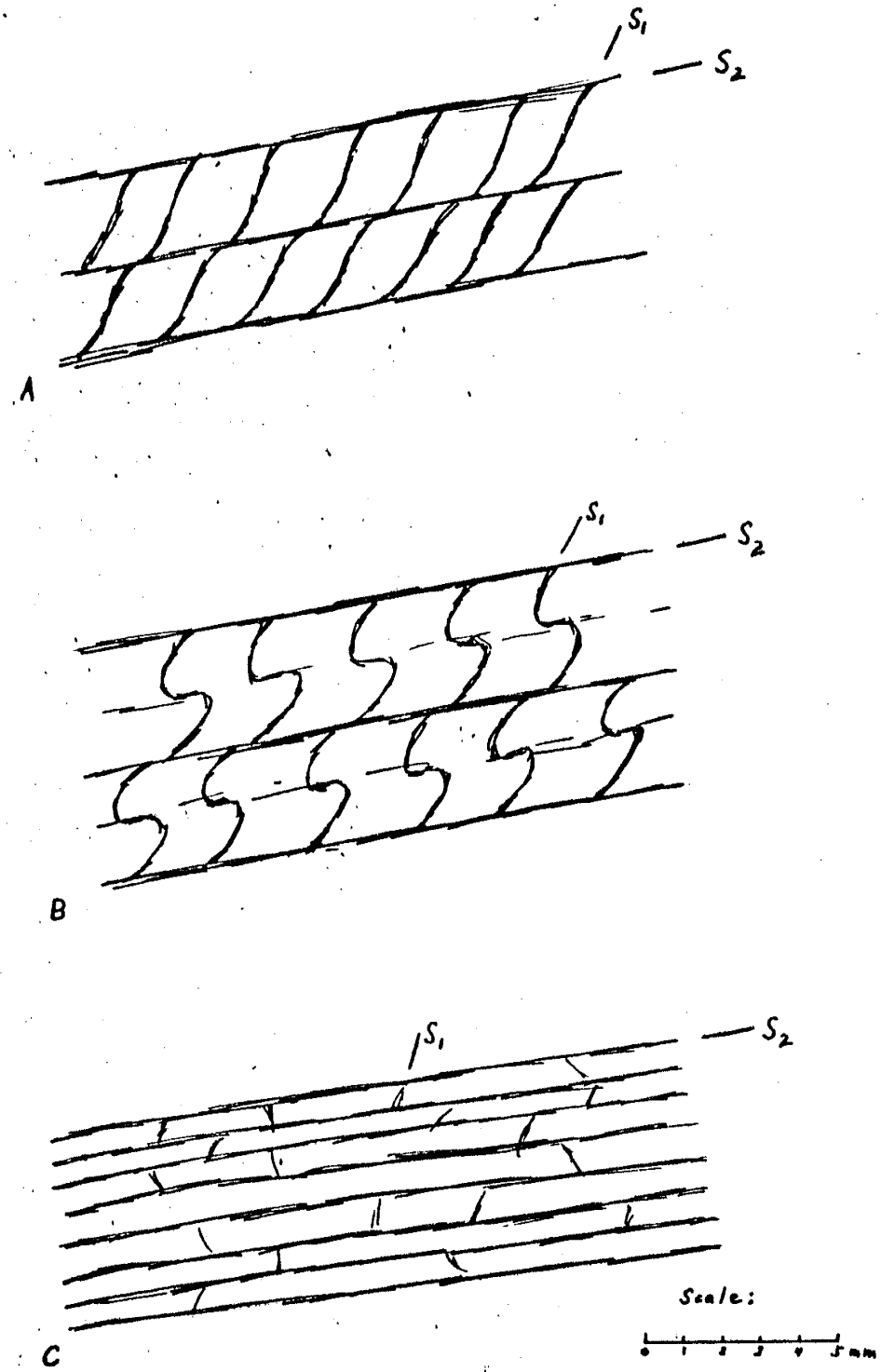

Figure 22. Successive stages, from A to C, in the formation of close-spaced S_2 slip cleavage.

symmetrical and assymmetrical flexural slip and cleavage folds. The style of these folds generally appears to be related to the lithology of the unit in which the folds occur. The sequence of photographs, Figures 28, 27, 26, 23 and 24, illustrates the changing style of F_2 folds with lithology and field location, from the leptynolite belt to White Ridge. Flexural slip folds without well-developed axial plane cleavage generally occur in leptynolite and muscovitic quartzite (Fig. 23), whereas chevron type cleavage folds with well-developed axial plane cleavage occur in feldspathic quartz-muscovite-chlorite and feldspathic quartz-muscovite-biotite schist (Fig. 24 and 25). Cleavage and flexural slip folds both occur sparsely in hornblende-chlorite schist. F_2 folds in muscovitic quartzite commonly occur as individual antiforms and synforms, as antiform-synform pairs with an amplitude of 6-15 inches (Fig. 26), or as small fold complexes. Less commonly, muscovitic quartzite is folded into large broad flexures as seen in Figure 27. Figure 27 also shows incipient development of axial plane cleavage to F_2 which is very rare in muscovitic quartzite. One of the rarely found F_2 folds in leptynolite is shown in Figure 28; this broad flexure fold has a sheared and crumpled axial area.

From the foregoing discussion it can easily be noted that the style, abundance and especially the orientation and the folded element are considerably different in F_1 and

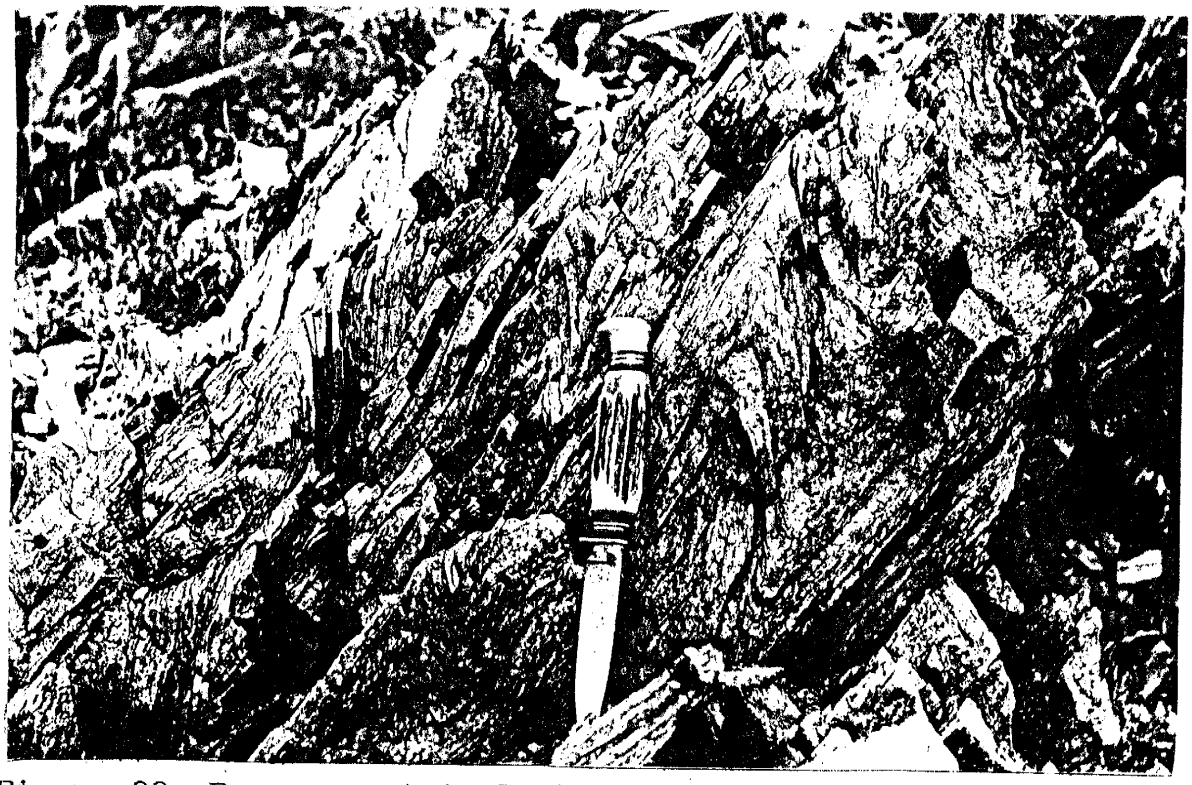

Figure 23. F_2 assymmetrical flexural slip folds with poorly developed axial plane cleavage in muscovitic quartzite; the folded element is S_1 axial plane cleavage.

Figure 24. F_2 chevron type cleavage folds folding S_1 in feldspathic quartz-muscovite-biotite schist.

Figure 25. Quartz layer defining F_2 folds in schist. S_2 axial plane cleavage is so well-developed in places that the folds are no longer recognizable.

Figure 26. F_2 antiform-synform pair in muscovitic quartzite.

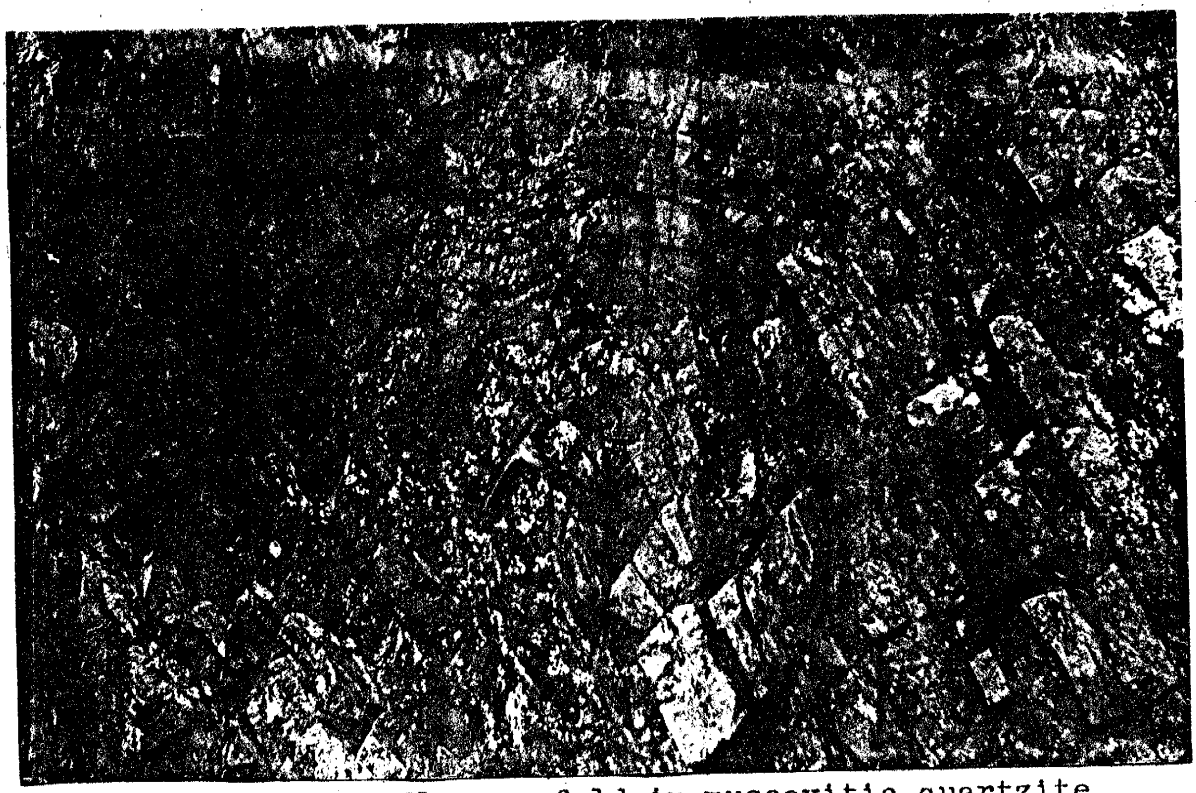

Figure 27. Broad F_2 flexure fold in muscovitic quartzite with incipient development of axial plane cleavage.

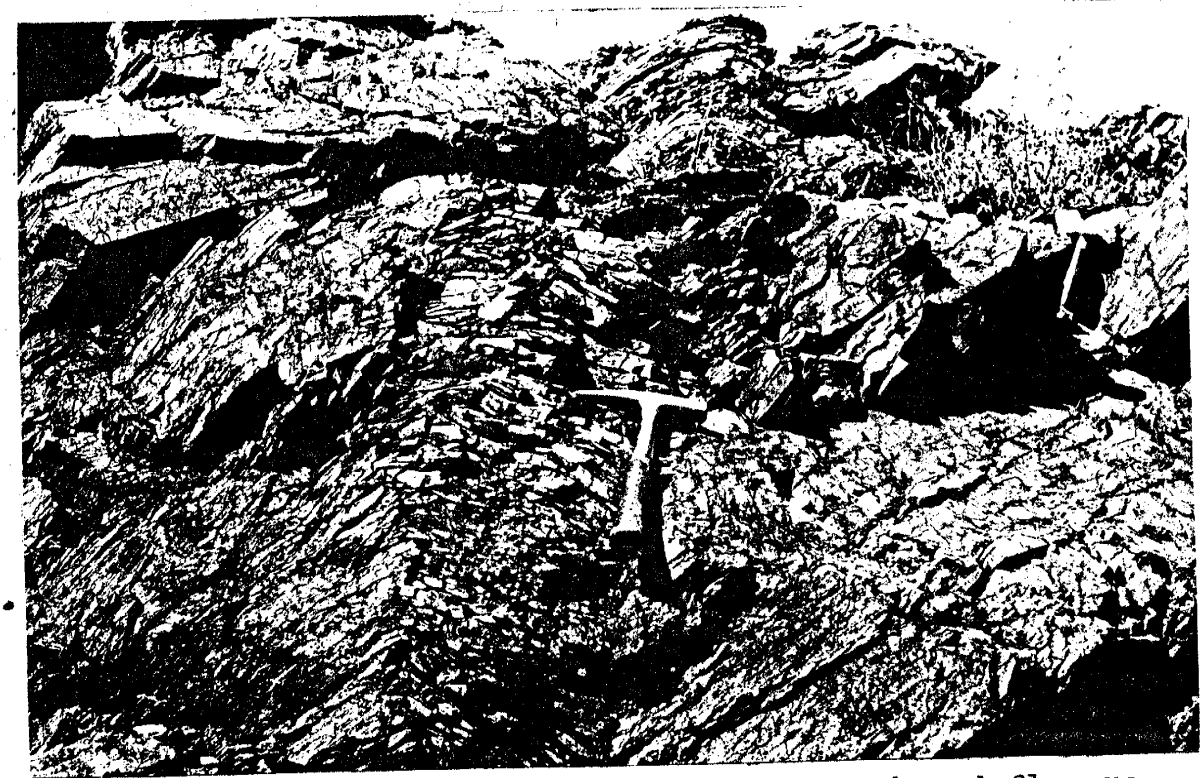

Figure 28. Rare F_2 fold in leptynolite; This broad flexure has folded S_1 axial plane cleavage. Note the crumpled and sheared axial area.

F_2 folds. This establishes the separation of D_1 from D_2.

Planar Structures

S_2 planar structures are slip cleavage and less commonly flow cleavage; both are axial plane cleavage to F_2 folds. S_2 cleavage is non-homogeneous and non-penetrative. It is best developed along White Ridge and in many outcrops of feldspathic quartz-muscovite-chlorite and feldspathic quartz-muscovite-biotite schist. The nature of exposures indicates that with increasing intensity of shearing, S_2 slip cleavage grades into F_2 chevron cleavage folding with S_2 as axial plane cleavage; S_2 slip cleavage in turn grades into pervasive S_2 flow cleavage. S_2 flow cleavage is developed to its greatest extent in the schist valley; however, F_2 chevron cleavage folds and S_2 slip cleavage also occur in the schist valley. Orientation of S_2 slip cleavage has been measured at 83 field stations. The strike of cleavage planes ranges from N 35^{o} W, through North, to N 70^{o} E (see Plate VI). Minor concentrations occur at N 25^{o}-45^{o} E, and N 15^{o}-20^{o} W. Dips average 40^{o}-60^{o} northerly and westerly, a few dipping easterly. Shear sense of S_2 slip cleavage is always noted on the S-shaped plane, looking down its plunge. No regular ordered distribution of right and left-handed shear sense is obvious except that the slip cleavages measured in the schist interlayers of the eastern belt of muscovitic quartzite have a greater percent of left-handed shears than those measured in other areas. S_2 flow

cleavage has the same general orientation as F_2 axial plane cleavage. Comparing S_2 slip cleavage planes, S_2 flow cleavage planes, and F_2 axial planes, it is perhaps significant to note that all of these D_2 cleavages have a considerable range in orientation and that all the orientations overlap. This heterogeneous orientation distinguishes S_2 cleavage from homogeneous S_1 cleavage.

Linear Structures

Intersecting planes, crinkles and fluting produce L_2 lineation. Intersection of S_2 cleavages and F_2 axial planes with S_1 planes produces the major type of L_2 lineation. The orientation of intersections of S_1 and S_2 is variable since S_2 orientation is variable. The bearing of this lineation ranges from N 30° E through North to S 15° W, with minor concentrations at N 30°-35° W and N 60° W. The plunge ranges from 35° to 70° northwest and southwest. The average plunge is about 35° NW. As noted in the section that describes F_2 folds, the F_2 fold axes have a wider range in orientation than the lineation just described. The concentrations of these two lineations overlap to a minor extent. L_2 lineation that is marked by crenulations and fluting has the same general trend as other L_2 lineations. Plate VII shows the wide range in orientation of L_2. Fluted and crenulated lineations are produced by small to microscopic flexing of S_1 flow cleavage.

The only other D_2 linear structures are boudin-shaped milky quartz segregations that occur in the noses of F_2 cleavage folds, and epidote pods that occur in axial areas of F_2 folds in hornblende-chlorite schist. Quartz boudins and segregations are most abundant at the contact between muscovitic quartzite and feldspathic quartz-muscovite-chlorite schist on White Ridge. Here the segregations are in the fold noses and the boudins trend parallel to F_2 axes.

THIRD DEFORMATION

Dislocation metamorphism, D_3, is the least pronounced of the three deformations recognizable in the northern part of the Los Pinos Mountains. The major product of D_3 is S_3 fracture cleavage which transects both S_1 and S_2 planes. L_3 is simple intersection of planar structures.

Microscopic Structures

S_3 fracture cleavage is present in the majority of thinsections examined for this report. In most slides S_3 is present as thin fractures that are oriented about 70° to 90° to S_1 and S_2. Individual fractures are spaced from 0.075mm to one centimeter apart. All grain boundaries are transected by S_3. Some of the fractures have been healed with secondary quartz. Some slides show only incipient development of S_3 fracture cleavage.

Mesoscopic Structures

Planar Structures

S_3 fracture cleavage is non-penetrative and homogeneous. It occurs as zones of close-spaced cleavage planes alternating with zones of very wide-spaced planes. Zones range in width from three inches to approximately 15 feet. In close-spaced cleavage zones individual planes range from less than one-half inch to three inches apart. S_3 planes are usually about eight inches to 15 inches apart in zones of wide-spaced fractures. S_3 planes generally strike East-West, but they do range from N 60° W to S 60° W (see Plate VIII). Dips are steep, commonly vertical. S_3 fracture cleavage transects all lithologic contacts and all older planar structures and folds.

Linear Structures

Intersection of S_3 with S_1 and S_2 produces lineation L_3 on S_3 planes. The orientation of L_3 has a considerable range due to the range in orientation of S_3 and S_2. L_3 generally bears to the north or northwest, ranging from N 20° E to N 30° W. This lineation commonly has a vertical plunge. L_3 lineation is one type of lineation that is always present since its nature is one of intersecting planes. However, L_3 is not always measureable due to the poor physical character of many outcrops.

JOINTS

In this report joints are termed S_4. S_4 joints are common in the map area and the orientations of joint planes were measured at more than 275 field stations. Three major S_4 joint sets have been recognized. The most conspicuous set is horizontal or nearly horizontal. Where this set is not horizontal it usually strikes in a northerly direction and dips generally from 5^{o} to 10^{o} to the east or west. The surfaces of this joint set commonly show well-developed feather fractures. Horizontal S_4 joints are not present along most of White Ridge in feldspathic quartz-muscovite-chlorite and feldspathic quartz-muscovite-biotite schist, but a moderately-spaced, horizontally oriented slip cleavage is developed. Outcrops in which this slip cleavage intersects older S-planes appear to have cleavage banding.

The other two S_4 joint sets occur at approximately 60^{o} - 70^{o} to each other. One set generally strikes N 25^{o} - 45^{o} W and dips about 80^{o} NE to 80^{o} SW. The strike of this set ranges from N 5^{o} W to N 85^{o} W with a minor concentration at N 40^{o} - 45^{o} W. The second set ranges in strike from N 5^{o} E to N 85^{o} E, but occurs mostly at N 25^{o} - 40^{o} E. Dips are mostly 30^{o} - 45^{o} southeastward but some are northwestward; the actural range in dip is from 15^{o} to 90^{o}.

All S_4 joints range from eight inches to 12 feet apart. The most common spacing is one to two feet. Separation along joint planes is usually less than two inches, and

mostly less than 1/8 inch. S_4 joints appear to cut all other structures in the map area, but it is often impossible to positively determine the cross-cutting relationships of planar elements such as S_4 joints and S_3 fracture cleavage.

SUMMARY OF STRUCTURAL GEOLOGY

Three periods of deformation have been recognized in the Precambrian rocks of the norhtern part of the Los Pinos Mountains. The deformations have produced various structural features that differ in style, orientation and order of superposition (see Table II for summary of structural geology).

The first recognizable deformation has transposed original compositional layering (bedding?). Intense componental slip movements have transposed original layering into tight isoclinal folds with well-developed axial plane cleavage that strikes N 20^{o} - 30^{o} E and dips 40^{o} - 70^{o} NW. Fold axes bear N 50^{o} - 70^{o} W and plunge 50^{o} - 70^{o} NW. Shearing has been so intense along the axial planes that most of the first deformation folds have been destroyed. Homogeneous and penetrative axial plane flow and fracture cleavage contains well-developed textural and mineralogic b-lineation.

Results of the second deformation include easily recognizable mesoscopic flexural slip and cleavage folds with axial plane cleavage that has a wide range in orientation. Well-developed slip and flow cleavage are also integral structures of the second deformation. Lineation has been

D_1	D_2	D_3
F_1: isoclinal flexure and shear folds. Folded element is compositional layering. N 50° - 70° W, 50° - 70° northwest.	F_2: symmetrical and assymmetrical flexural slip and cleavage folds. Folded element is S_1. N 25° E to S 15° W, 35° - 60° north & west.	NO FOLDS.
S_1: homogeneous and penetrative, axial plane flow and fracture cleavage N 20° - 30° E, 40°-70° NW.	S_2: non-homogeneous, non-penetrative, axial plane flow, fracture, and slip cleavage. N 35° W to N 70° E, 40° - 60° north & west.	S_3: homogeneous and non-penetrative; close-spaced and wide-spaced fracture cleavage. East - west trending, steeply dipping.
L_1: mineralogic and textural b-lineation. N 60°-85° W, 50°-80° NW	L_2: intersection of S_1 and S_2, and fluting. N 30° E to S 15° W, 35°-70° north- and south-westerly.	L_3: intersection of S_3 with S_1 and S_2. bearing northwesterly, plunging steeply.

TABLE II. Summary of Structural History

produced by crinkling, fluting and intersecting planes.

The third deformation has resulted in non-homogeneous and penetrative fracture cleavage which trends east-west and dips steeply. This cleavage occurs in alternating zones of close-spaced and wide-spaced fractures. Lineation is produced by intersection of fracture cleavage with older planar structures.

Jointing appears to be the youngest structural feature of the map area. Three sets of joints have been recognized: (1) a horizontally trending set, (2) a N 30° - 35° E trending set that dips 50° - 60° NW to SE and (3) a N 30° - 35° W trending set that dips 35° - 40° NE to SW.

Order of superposition of structural elements and style are major criteria for separating periods of deformation. There is no known way of estimating the elapsed time between each deformation, nor the duration of each deformation. Radiogenic dating may be useful but could easily be unsatisfactory due to isotope modification during one or all deformations, or lack of isotope modification in purely mechanical deformations.

GEOLOGIC HISTORY

1. Deposition of sediments with possible intervals of extrusion (and intrusion) of volcanic rocks to form a layered lithologic sequence.

2. Intrusion (?) of granitic rock.

3. First metamorphic period consisted of homogeneous and penetrative deformation accompanied by mineralogic reconstitution. Results of this period were a northeast trending system of isoclinal shear folds, and recrystallization of equilibrium mineral assemblages in a pressure-temperature environment similar to that of the greenschist and almandine-amphibolite facies. Characteristic products of this event were phyllites (phyllonites?), schists and gneiss.

4. Thermal metamorphism with no obvious componental movement resulted in the crystallization of large biotite and chlorite flakes.

5. Cataclastic (?) metamorphism produced a system of flexural slip and cleavage folds and non-homogeneous, non-penetrative slip and flow cleavage with a wide range in orientation. Recognizable mineralogic reconstitution did not occur during this event.

6. Dislocation metamorphism produced non-homogeneous, penetrative fracture cleavage, trending east-west and dipping steeply.

7. Retrograde metamorphism resulted in the recrystallization of chlorite from biotite. (This event could have been associated with event #5 or #6).

8. Erosion to the Precambrian rocks.

9. Local deposition of conglomerate on the Precambrian surface.

10. Deposition of some Paleozoic (Pennsylvanian) sediments.

11. Thrusting of Precambrian metamorphics over Pennsylvanian sediments.

12. Normal faulting related to the Rio Grande graben structure.

13. Erosion to the present time and formation of the Tio Bartolo Pediment.

GLOSSARY

Antiform is a fold closing upward with unknown or no stratigraphic features, e.g. folds in foliation, (Turner and Weiss, p.106; Bailey, p.121, 1939).

Axial plane cleavage is that cleavage which is parallel to the axial plane of a fold (Turner and Weiss, p.99).

B-lineation: using Sander's terminology where the tectonic b-axis is the axis of external rotation, a b-lineation in the classical sense is that lineation which is parallel to a fold axis.

Flow cleavage is "the cleavage dependent on the parallel arrangement of the mineral constituents of the rock" (Leith, p.23, 1905). Minerals that define flow cleavage in rocks of the map area are mica and hornblende.

Fracture cleavage "is a parting defined by closely-spaced discrete parallel fractures ideally independent of any planar preferred orientation of grain boundaries that may exist in the rock" (Turner and Weiss, p.98, 1963). Leith (1905) said that fracture cleavage is a structure which develops in shearing planes.

Homogeneity of structures occurs when "samples compared are sufficiently large in relation to structural heterogeneities, so that each sample contains a representative distribution of these heterogeneities. Such samples are statistically identical and the body (or structure) concerned is "said to be "statistically homogeneous." (Turner and Weiss, p.16-17). Structural homogeneity implies identity with respect to all possible structural features in a rock body, or to specific geometric features of the body. So if a rock body has a planar element, e.g. flow cleavage, that is statistically present everywhere on a certain scale, the rock body is structurally and statistically homogeneous with respect to the flow cleavage.

Lineation according to Cloos (1946) is "... a descriptive and non-genetic term for any kind of linear structure within or on a rock. It includes striae on slickensides, fold axes, flow lines, stretching, elongated pebbles or ooids, wrinkles, streaks, intersection of planes, linear parallelism of minerals or components, or any other kind of linear structure of megascopic, microscopic or regional dimensions." In this report the term lineation is restricted to linear structures penetrative in hand specimen or small exposures.

Penetrative: structures are called penetrative if they occur repeatedly at distances so small compared with the scale of the rock body that they can be considered to pervade the rock body uniformly and be present at every point in the rock body (Turner and Weiss, p.21-31).

Schistosity is used synonymously with flow cleavage in this report.

Slip cleavage (or strain-slip cleavage) is a variety of fracture cleavage which develops in micaceous rocks (Leith, 1905). It is a cleavage "defined by parallel narrow domains or discrete surfaces of incipient transposition of a pre-existing foliation " (Turner and Weiss, p.98; Leith, 1905; Harker, 1932). Slip cleavage generally produces micro-drag folds, crenulations, waves and wrinkles. "Fracture cleavage in one type of rock may be synchronous with and dynamically equivalent to strain-slip cleavage in associated beds of another type" (Turner and Weiss, p.98).

Structures: structural discontinuties in a rock body are here referred to as structures, e.g. flow cleavage, fracture cleavage and lineation.

Synform is a fold closing downward with unknown or no stratigraphic features (Turner and Weiss, p.106;Bailey, p.121, 1939).

The use of letters for structural features follows Sander (1930), Fairbairn (1949) and Turner and Verhoogen (1960). "D" denotes a deformational period, "L" indicates any lineation, "S" refers to any planar structure, and "F" indicates a fold. Numerical subscripts of "D" refer to different periods of deformation from the oldest recognizable period, D_1, to the youngest, D_3. The use of S_0 for a planar element which predates S_1 but for which there is no recognizable deformation, permits the use of the same numerical subscripts for all structural elements formed during a particular deformation; thus S_1, L_1 and F_1 are products of D_1.

BIBLIOGRAPHY

Bailey, E.B., in E.B. Bailey, J.Weir, and W.J. McCallien (1939) Introduction to Geology, London: Macmillan, 121p.

Bingler, E.C. (1965) Precambrian geology of La Madera quadrangle, Rio Arriba County, New Mexico, N. Mex. Inst. Min. and Tech., State Bur. Mines and Mineral Res., Bull. 80.

Brown, W.L. in Pitcher, W.S., and Flinn, G.W. (editors) (1965) Controls of Metamorphism, New York: John Wiley and Sons, Inc., 368p.

Cloos, Ernst (1946) Lineation: A critical review and annotated bibliography, Geol. Soc. Am., Mem. 18, 122p.

Denny, Charles S. (1941) Quaternary geology of the San Acácia area, New Mexico, Jour. Geol., v. 49, p.225-260.

Fairbairn, H.W. (1949) Structural petrology of deformed rocks, Cambridge, Mass.: Addison-Wesley Pub. Co., 344p.

Freedman, J., Wise D.U., and Bentley, R.D. (1964) Pattern of folded folds in the Appalachian Piedmont along Susquehana River, Geol. Soc. Am. Bull., v.75, p.621-638.

Fyfe, W.S., Turner, F.J., and Verhoogen, J. (1958) Metamorphic reactions and metamorphic facies, Geol. Soc. Am., Mem. 73, 259p.

Harker, A. (1932) Metamorphism, London: Meuthen, 203p.

Knopf, E.B. (1931) Retrogressive metamorphism and phyllonitization, Am. Jour. Sc., v. 21, p.1-27.

Leith, C.K. (1905) Rock cleavage, U.S. Geol. Surv., Bull.239, 216p.

Nelson, B.W. , and Roy, R. (1958) Synthesis of the chlorites and their structural and chemical composition, Am. Min., v. 43, p.707-725.

Reiche, Parry (1949) Geology of the Manzanita and North Manzano Mountains, New Mexico, Geol. Soc. Am. Bull., v. 60, p.1183-1212.

Sander, B. (1930) Gefugekunde der Gertein, Vienna: Springer, 352p.

Staatz, M.H., and Norton, J.J., (1942) The Precambrian geology of the Los Pinos Range, New Mexico, unpublished M.S. thesis, Northwestern University, 150p.

Stark, J.J. (1956) Geology of the South Manzano Mountains, New Mexico, N. Mex. Inst. Min. and Tech., State Bur. Mines and Mineral Res., Bull. 34.

_____, and Dapples, E.C.(1946) Geology of the Los Pinos Mountains, New Mexico,Geol. Soc. Am. Bull., v.57, p.1121-1172.

Tilley, C.E. (1926) Some mineralogical transformations in crystalline schists, Min. Mag., v.21, 34p.

Turner, F.J., and Verhoogen, J. (1960) Igneous and metamorphic petrology, New York: McGraw-Hill Book Co., Inc. (2nd ed.), 694p.

_____, and Weiss, L.E. (1963) Structural analysis of metamorphic tectonites, New York: McGraw-Hill Book Co., Inc., 545p.

Williams, H., Turner, F.J., and Gilbert, C.M. (1954) Petrography: An introduction to the study of rocks in thinsection, San Francisco: W.H. Freeman and Co., 406p.

This thesis is accepted on behalf of the faculty of the Institute by the following committee:

Edward A. Bryden

Mary E. Willard

Clay T. Smith

L. R. Hathaway

Date: 5 May 1966

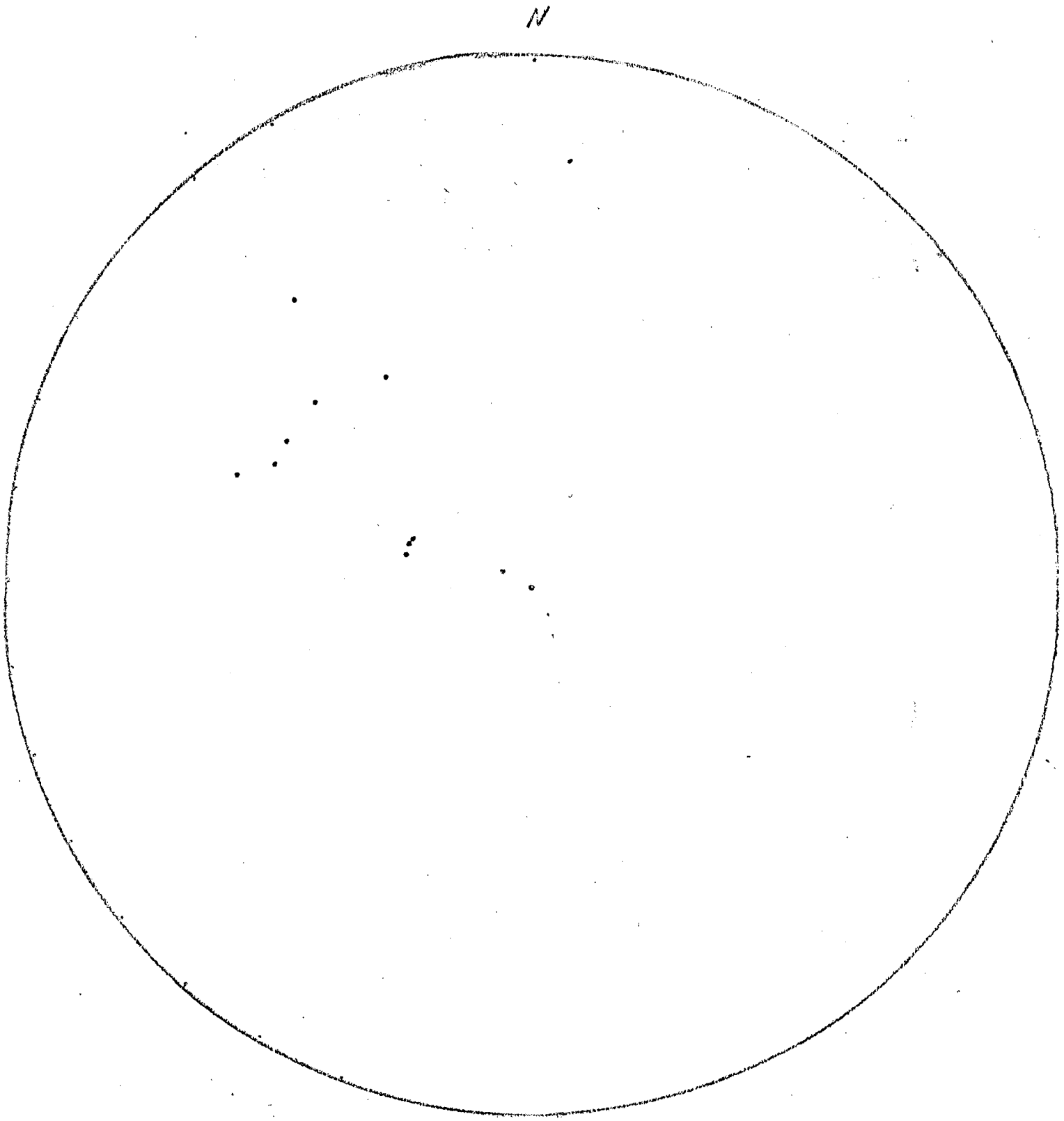

Plate II. Twelve mesoscopic F_1 fold axes

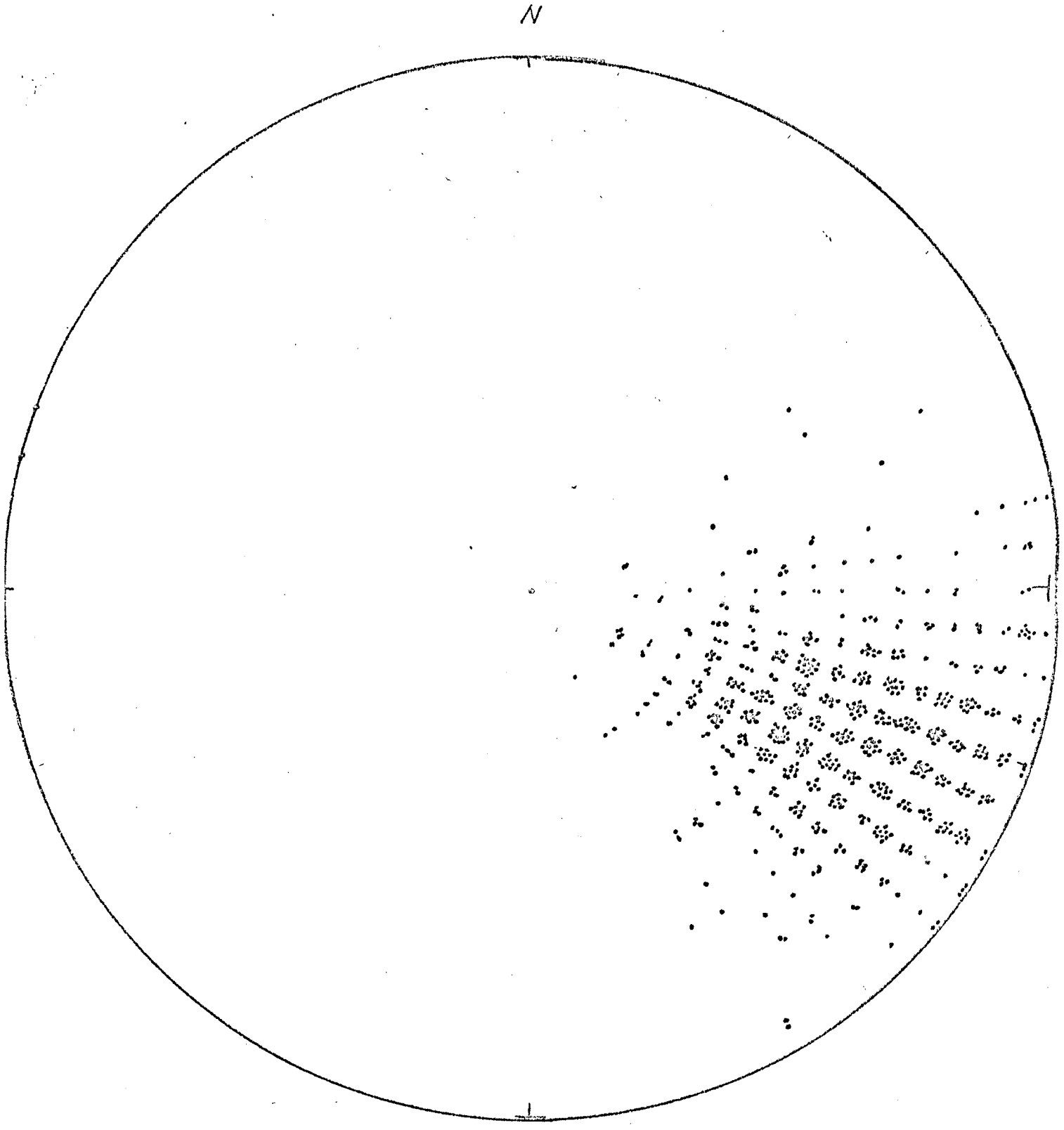

Plate III. 702 poles to S_1 axial plane flow and fracture cleavage.

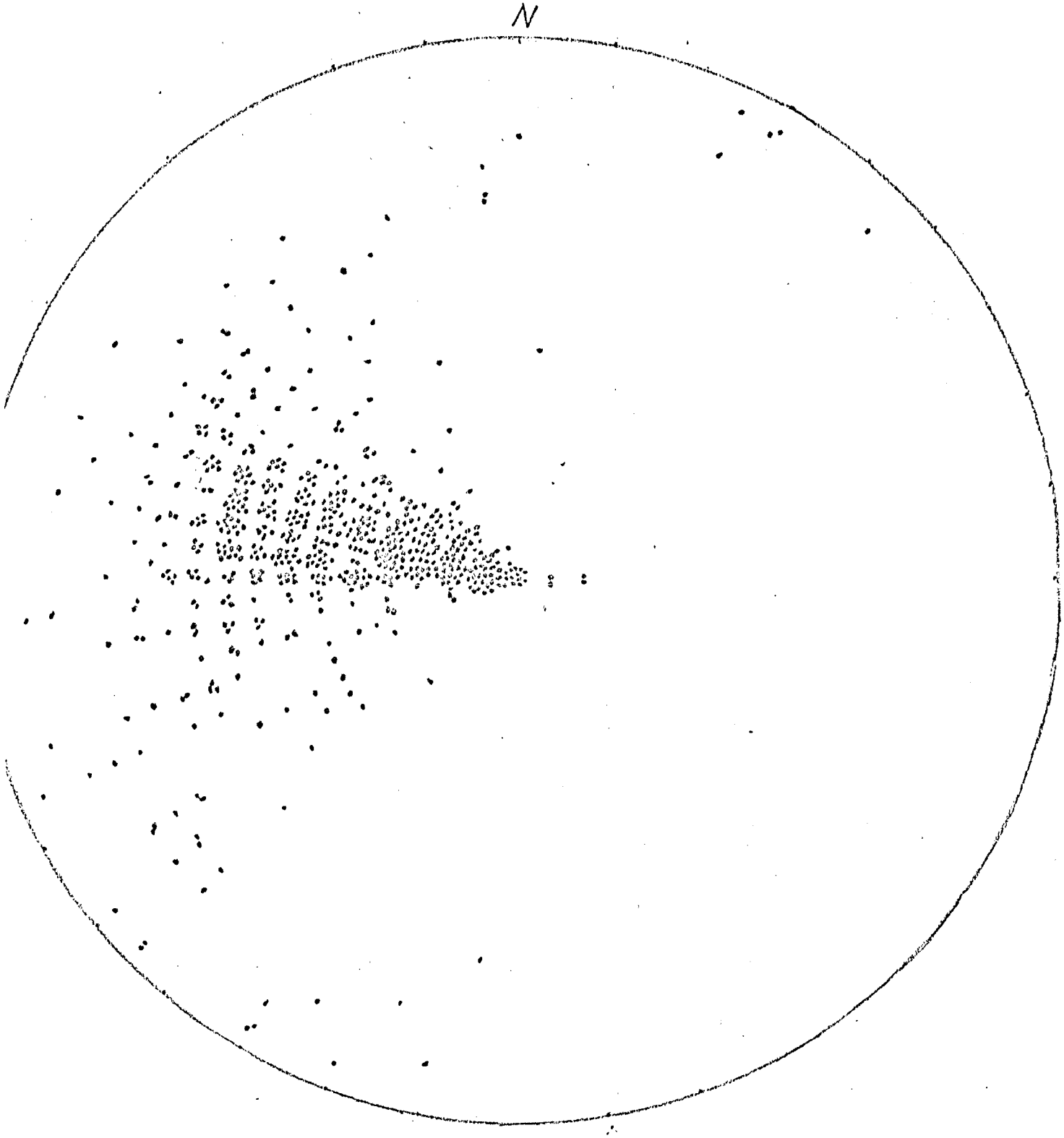

Plate IV. 690 mineralogic and textural L_1 lineations.

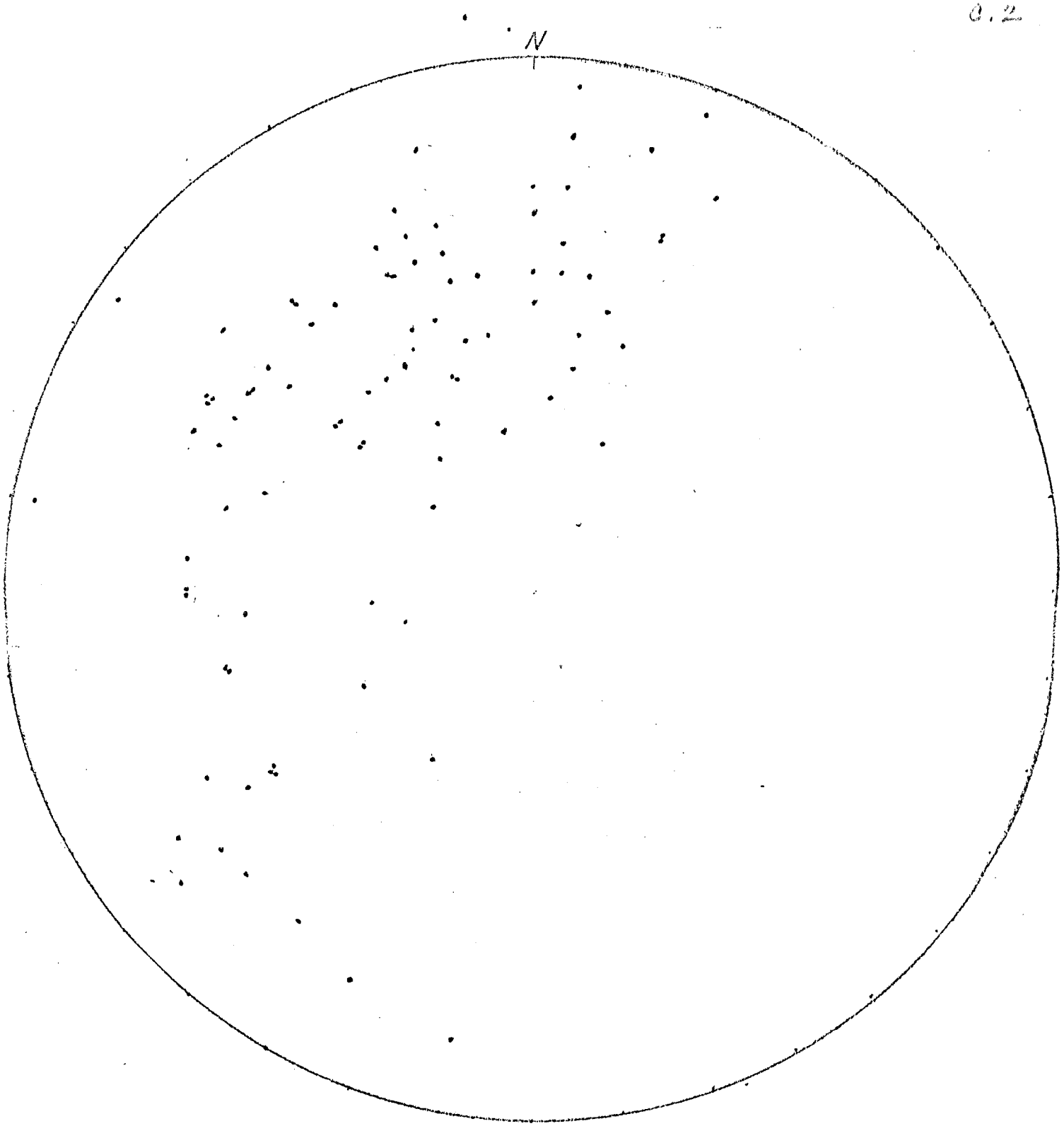

Plate V. 90 mesoscopic F_2 fold axes.

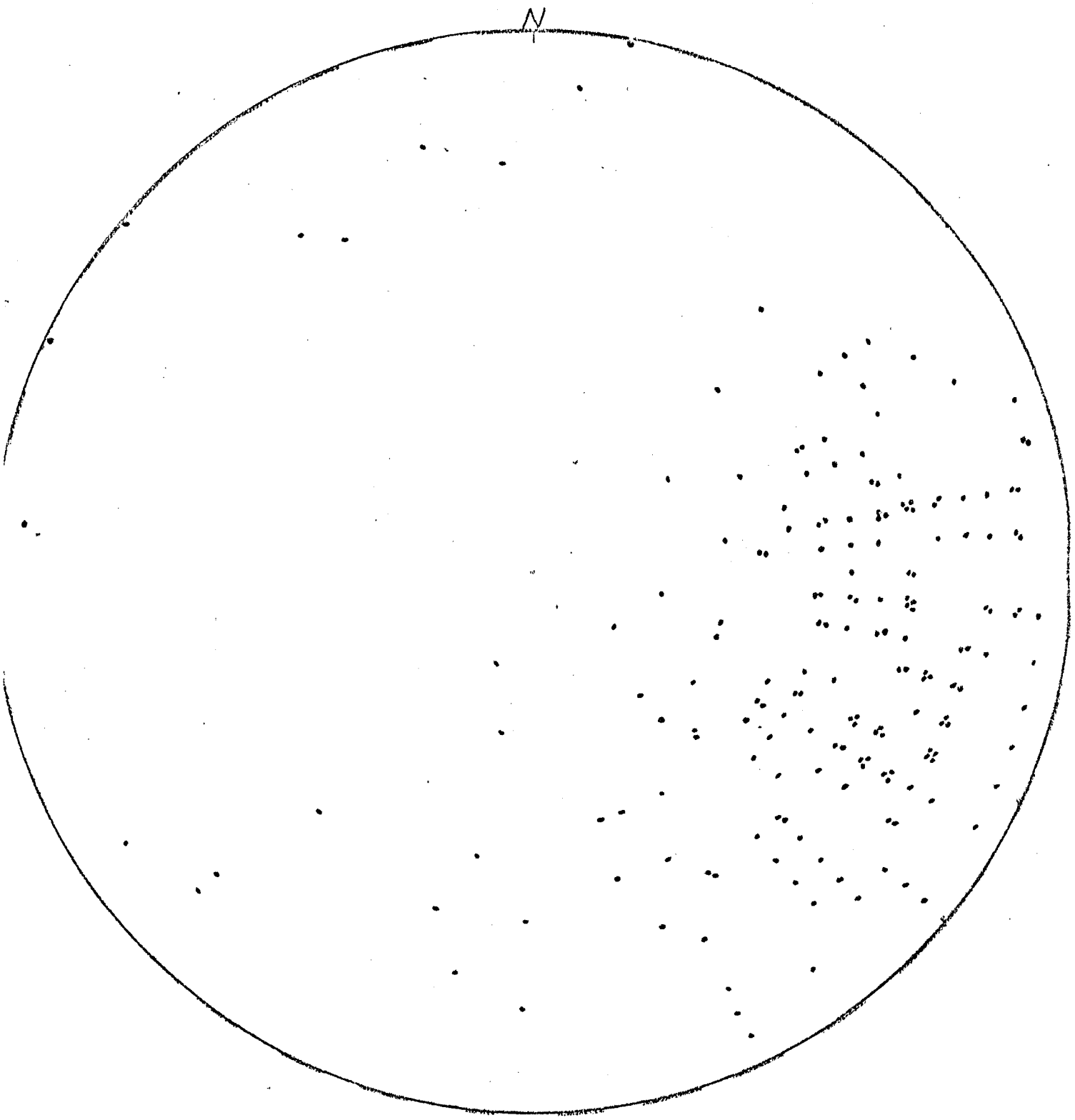

Plate VI. 173 poles to S_2 axial plane flow, fracture and slip cleavage.

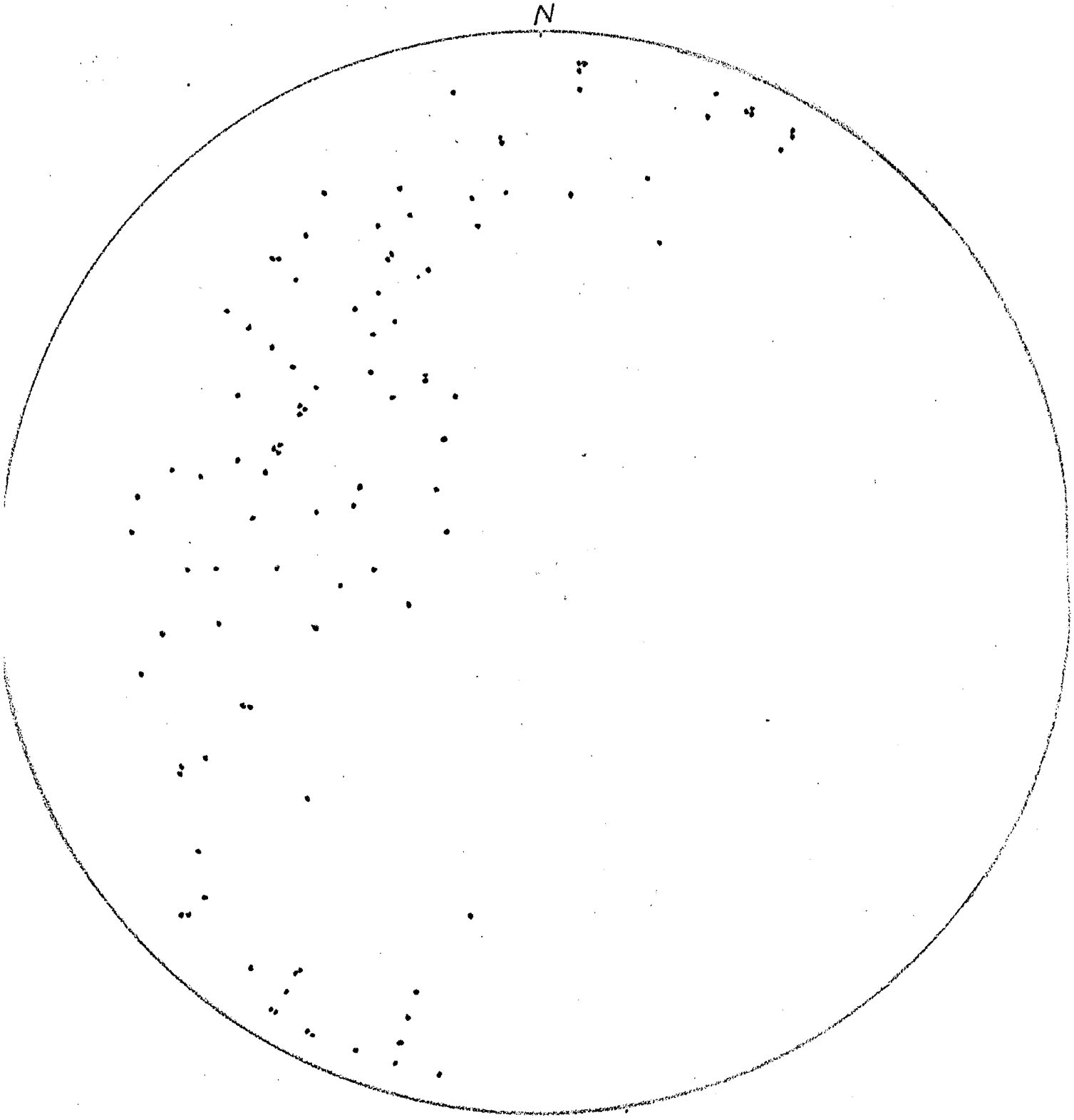

Plate VII. 101 L_2 lineations produced by intersection of planes and crinkling.

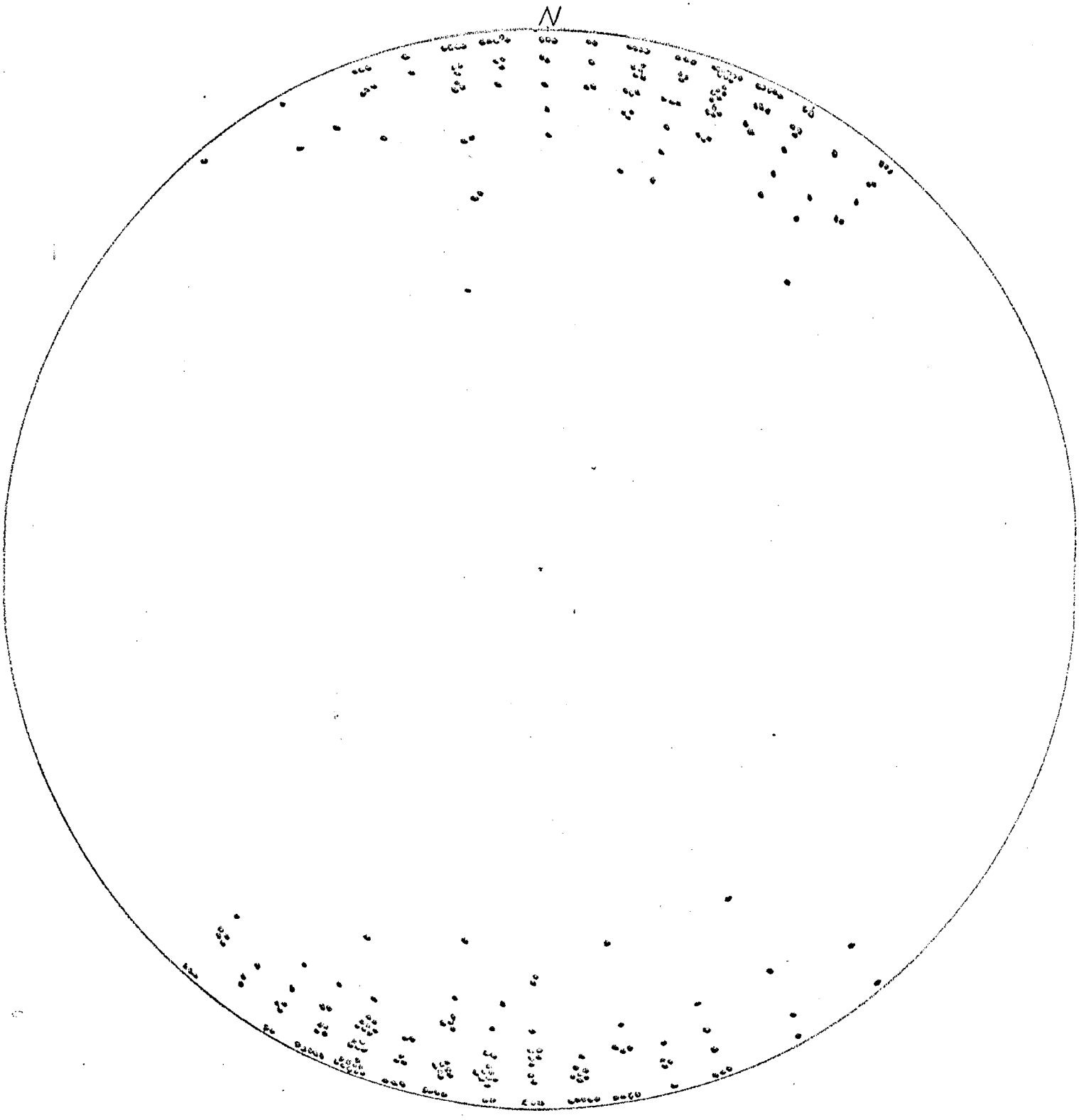

Plate VIII. 235 poles to S_3 fracture cleavage.